UNCLASSIFIED

SECURITY CLASSIFICATION OF THIS PAGE

REPORT DOCUMENTATION PAGE

1a. REPORT SECURITY CLASSIFICATION UNCLASSIFIED	1b. RESTRICTIVE MARKINGS
2a. SECURITY CLASSIFICATION AUTHORITY	3. DISTRIBUTION / AVAILABILITY OF REPORT Approved for public release; distribution is unlimited.
2b. DECLASSIFICATION / DOWNGRADING SCHEDULE	
4. PERFORMING ORGANIZATION REPORT NUMBER(S) NSWC TR 88-6	5. MONITORING ORGANIZATION REPORT NUMBER(S)
6a. NAME OF PERFORMING ORGANIZATION Naval Surface Warfare Center 6b. OFFICE SYMBOL (If applicable) U13	7a. NAME OF MONITORING ORGANIZATION
6c. ADDRESS (City, State, and ZIP Code) 10901 New Hampshire Avenue Silver Spring, MD 20903-5000	7b. ADDRESS (City, State, and ZIP Code)
8a. NAME OF FUNDING / SPONSORING ORGANIZATION 8b. OFFICE SYMBOL (If applicable)	9. PROCUREMENT INSTRUMENT IDENTIFICATION NUMBER
8c. ADDRESS (City, State, and ZIP Code)	10. SOURCE OF FUNDING NUMBERS PROGRAM ELEMENT NO. N/A; PROJECT NO. 4U91VB; TASK NO. N/A; WORK UNIT ACCESSION NO. N/A

11. TITLE (Include Security Classification)
NOTES ON A THEORETICAL PARACHUTE OPENING FORCE ANALYSIS APPLIED TO A GENERAL TRAJECTORY

12. PERSONAL AUTHOR(S)
William P. Ludtke

13a. TYPE OF REPORT	13b. TIME COVERED	14. DATE OF REPORT (Year, Month, Day)	15. PAGE COUNT
Final	FROM 1987 TO 1988	88/5/28	

16. SUPPLEMENTARY NOTATION

17. COSATI CODES			18. SUBJECT TERMS (Continue on reverse if necessary and identify by block number)
FIELD	GROUP	SUB-GROUP	Variable Deployment Angle; Opening Shock; Inflation Time; Calculation Methods; Parachute Technology; Altitude Effects
01	03		

19. ABSTRACT (Continue on reverse if necessary and identify by block number)

This report presents a method for calculating the inflation reference time and opening shock forces of the solid-cloth family of parachutes when deployed at an arbitrary trajectory angle to the horizontal.

The method is extended to other types of parachutes, but it is limited in that the inflation reference times are not calculated as part of the deployment process. Particular inflation times must be provided as input data to the furnished computer program. The variation of opening shock force versus inflation reference time may be surveyed by providing several values or using actual field test data.

Examples are used to demonstrate the effects of canopy cloth rate of airflow, altitude, and trajectory deployment angle for constant velocity

20. DISTRIBUTION / AVAILABILITY OF ABSTRACT ☒ UNCLASSIFIED/UNLIMITED ☐ SAME AS RPT. ☐ DTIC USERS	21. ABSTRACT SECURITY CLASSIFICATION UNCLASSIFIED
22a. NAME OF RESPONSIBLE INDIVIDUAL William P. Ludtke	22b. TELEPHONE (Include Area Code) (202) 394-1705 22c. OFFICE SYMBOL U13

DD FORM 1473, 84 MAR — 83 APR edition may be used until exhausted. All other editions are obsolete

SECURITY CLASSIFICATION OF THIS PAGE

☆ U.S. Government Printing Office: 1986—607-044

19. and constant dynamic pressure-altitude profiles.

NSWC TR 88-6

NOTES ON A THEORETICAL PARACHUTE OPENING FORCE ANALYSIS APPLIED TO A GENERAL TRAJECTORY

BY WILLIAM P. LUDTKE

UNDERWATER SYSTEMS DEPARTMENT

28 MAY 1988

NAVAL SURFACE WARFARE CENTER

Dahlgren, Virginia 22448-5000 • Silver Spring, Maryland 20903-5000

FOREWORD

This report presents a method for calculating the inflation reference time and opening shock forces of the solid-cloth family of parachutes when deployed at an arbitrary trajectory angle to the horizontal.

The method is extended to other types of parachutes, but it is limited in that the inflation reference times are not calculated as part of the deployment process. Particular inflation times must be provided as input data to the furnished computer program. The variation of opening shock force versus inflation reference time may be surveyed by providing several values or using actual field test data.

Examples are used to demonstrate the effects of canopy cloth rate of airflow, altitude, and trajectory deployment angle for constant velocity and constant dynamic pressure-altitude profiles.

The author wishes to express his appreciation to Mr. Hensel Brown of the Strategic Systems Department for his valuable assistance. Mr. Brown developed the computer programs and conducted numerous background calculations for this report.

Approved by:

DR. J. E. GOELLER, Head
Underwater Weapons Division

CONTENTS

ILLUSTRATIONS

TABLES

INTRODUCTION

Studies of parachute opening shock force in the horizontal and vertical deployment modes are particular solutions to a difficult problem. Often stores are launched in loft or dive modes. Other stores may be launched horizontally, but retarder deployment is delayed until such time as neither the closed mode horizontal analysis or the vertical approach is applicable. In this report an opening shock force technique is developed for a generalized trajectory angle at deployment. A method for calculating the inflation time of solid-cloth parachutes is presented by way of Mode 1 of a two-mode computer program. Mode 2 of the computer program is applicable to other types of parachutes where the inflation reference time is known or can be assumed and varied.

APPROACH

The analysis is based upon the application of Newton's second law of motion to particle trajectories of inflating parachutes deployed at arbitrary angles to the horizontal plane. Equations for the horizontal deployment of parachutes with a dynamic drag area signature of the form $C_DS/C_DS_O = (1-\tau)(t/t_o)^j + \tau$ was developed in Reference 1. The same drag area signature was incorporated into the vertical toward-the-earth trajectory of Reference 2. The exponent j determines the type of parachute. A value of j=1 is indicative of geometrically porous ribbon and ring slot types of canopies. Solid-cloth parachutes have a value of j=6.

C_DS = Instantaneous parachute drag area during inflation

C_DS_O = Steady state drag area of the fully inflated parachute

τ = The ratio of the parachute drag area at t=0 to the steady state parachute drag area, $\tau = C_DS_i/C_DS_O$

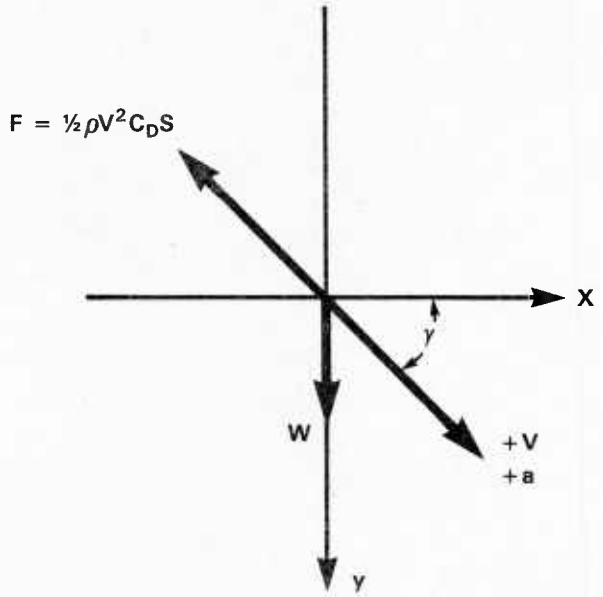

FIGURE 1. ARBITRARY TRAJECTORY ANGLE POINT MASS FORCE SYSTEM

DEVELOPMENT OF THE VELOCITY-TIME EQUATION AND OPENING SHOCK FORCE
With reference to Figure 1.

$$\Sigma F_x = ma_x \qquad \Sigma F_y = ma_y$$

$$-\frac{1}{2}\rho V^2 C_D S \cos\gamma = \frac{W}{g}\frac{\Delta V_x}{\Delta t} \qquad W - \frac{1}{2}\rho V^2 C_D S \sin\gamma = \frac{W}{g}\frac{\Delta V_y}{\Delta t}$$

$$\Delta V_x = \frac{-g\rho V^2 C_D S \cos\gamma}{2W}\Delta t \quad (1) \qquad \Delta V_y = \left(g - \frac{g\rho V^2 C_D S \sin\gamma}{2W}\right)\Delta t \quad (2)$$

$$C_D S = C_D S_o\left((1-\tau)\left(\frac{t}{t_o}\right)^j + \tau\right) \quad (3)$$

$$\Delta V_x = \left(-\frac{V_s t_o}{V_s t_o} \times \frac{g\rho V^2 C_D S_o\left((1-\tau)\left(\frac{t}{t_o}\right)^j + \tau\right)\cos\gamma}{2W}\right)\Delta t \qquad \Delta V_y = \left(g - \frac{V_s t_o}{V_s t_o} \times \frac{g\rho V^2 C_D S_o\left((1-\tau)\left(\frac{t}{t_o}\right)^j + \tau\right)\sin\gamma}{2W}\right)\Delta t$$

AT $t = 0$

$$\text{LET } M = \frac{2W}{\rho g V_s t_o C_D S_o} \quad (4)$$

$$\text{LET } \Delta t = \text{TIME STEP} = \frac{t_o}{100{,}000}$$

$$V_x = V_s \cos\gamma$$

$$V_y = V_s \sin\gamma$$

AT THE TIME t

$$\sum_{V_x = V_s\cos\gamma}^{V_x} \Delta V_x = \sum_{t=o}^{t}\left(\frac{-V^2\left((1-\tau)\left(\frac{t}{t_o}\right)^j + \tau\right)\cos\gamma}{MV_s t_o}\right)\Delta t \quad (1a) \qquad \sum_{V_y = V_s\sin\gamma}^{V_y} \Delta V_y = \sum_{t=o}^{t}\left(g - \frac{V^2\left((1-\tau)\left(\frac{t}{t_o}\right)^j + \tau\right)\sin\gamma}{MV_s t_o}\right)\Delta t \quad (2a)$$

Where the quantity $2W/(\rho g V_s t_o C_D S_o)$ has been shown in Reference 1 to be a Ballistic Mass Ratio (BMR) scale factor.
The trajectory velocity, V:

$$V = \sqrt{V_x^2 + V_y^2} \tag{5}$$

the trajectory angle, γ :

$$\text{Tan}\,\gamma = \frac{V_y}{V_x} \tag{6}$$

At any instant during the inflation process the shock factor has been shown in Reference 1 to be:

$$\chi_i = \left(\frac{V}{V_s}\right)^2 \frac{C_D S}{C_D S_o} \tag{7}$$

and the instantaneous shock force is:

$$F_i = \chi_i F_s \tag{8}$$

where F_s is the steady-state drag force of the fully open parachute at the line stretch velocity, V_s.

$$F_s = \tfrac{1}{2}\rho V_s^2 C_D S_o \tag{9}$$

DEVELOPMENT OF THE INFLATION REFERENCE TIME EQUATION FOR SOLID-CLOTH PARACHUTES

The solid-cloth parachute inflation reference time "t_o" in the arbitrary trajectory angle mode can be determined from the basic mass flow equation used to calculate the horizontal deployment "t_o". Following the method of Section IV of Appendix A for solid-cloth parachutes. Appendix B is included as a guide to assist in the use of Appendix A in the solution of particular problems. Refer to page A-16 for nomenclature definitions.

A program for calculating t_o for solid-cloth parachutes and the opening shock force profile during the inflation of several parachute types is provided in Table 1. Equations (1a) through (11) are programmed together with the opening shock equations (7) through (9) in FORTRAN IV language. The included examples were calculated via the program using a VAX 780 computer. The program operates in two modes. Mode 1, for solid-cloth parachutes, calculates the deployment inflation reference time t_o for the parachute system parameters and operational deployment data, and also calculates the opening shock profile during inflation. A typical data print out is shown in Table 2. It is necessary to estimate an initial value of "t_o". The program calculates the canopy volume for the estimated time and compares the $V_{o\ calc}$ to the volume derived from the canopy geometry. If the calculated

$d_m = m_{inflow} - m_{outflow}$ where m refers to mass of air flowing

$$\rho \frac{dV}{dt} = \rho V A_m - \rho A_s P$$

Instantaneous canopy mouth area.

$$A_m = A_{mo}\left(\frac{t}{t_o}\right)^6 \qquad \text{FOR } \tau = 0$$

Instantaneous pressurized canopy cloth area.

$$A_s = A_{so}\left(\frac{t}{t_o}\right)^6 \qquad \text{FOR } \tau = 0$$

Instantaneous cloth rate of airflow.

$$P = k\left(\frac{C_p\,\rho}{2}\right)^n V^{2n} \qquad \text{C.F.S./FT}^2$$

Where the instantaneous velocity is determined by equation (5) for $\tau = 0$.
The calculated canopy volume $V_{o\ calc}$, is determined from equation (10).

$$V_{o\,calc} = \sum_{V=o}^{V_o} \Delta V = \sum_{t=o}^{t_o} \left[VA_{mo}\left(\frac{t}{t_o}\right)^6 - A_{so}\left(\frac{t}{t_o}\right)^6 k\left(\frac{C_p\,\rho}{2}\right)^n V^{2n} \right] \Delta t \qquad (10)$$

TABLE 1. PARACHUTE PROGRAM

```
C*************************************************************************
C  THIS PROGRAM CALCULATES INSTANTANEOUS VELOCITY, DISTANCE OF FALL,     *
C  DRAG AREA, AND OPENING SHOCK FORCE OF A PARACHUTE DEPLOYED IN         *
C  ANY DIRECTION.                                                        *
C*************************************************************************
C
C  THE PROGRAM OPERATES IN TWO MODES:
C
C   MODE 1 - CALCULATES THE INFLATION TIME AND PERFORMANCE PROFILES FOR
C            SOLID-CLOTH PARACHUTES (TO INPUT AS INITIAL ESTIMATE)
C            (IOPT=1)
C
C   MODE 2 - CALCULATES THE PERFORMANCE PROFILES FOR VARIOUS TYPES OF
C            PARACHUTES (J).  INFLATION TIME IS REQUIRED AS INPUT.
C            (IOPT=2)
C
C*************************************************************************
C
C  INPUT NEEDED FOR BOTH MODES:
C
C          ALT   -  ALTITUDE. (FT)  NOT USED IN ANY CALCULATIONS.
C          RHO   -  AIR DENSITY AT GIVEN ALTITUDE. (SLUGS/FT3)
C           VS   -  VELOCITY AT SUSPENSION LINE STRETCH. (FT/SEC)
C         CDSO   -  DESIGN DRAG AREA. (FT2)
C           TO   -  IOPT=1  INITIAL GUESS FOR INFLATION REF. TIME. (SEC)
C                   IOPT=2  ACTUAL INFLATION REFERENCE TIME.  (SEC)
C            W   -  WEIGHT  (LBS)
C            J   -  =6 FOR FLAT CIRCULAR PARACHUTE.
C                   =1 FOR RIBBON TYPE OF PARACHUTE.
C          TAU   -  INITIAL DRAG-AREA RATIO.
C     ALPHA(0)   -  INITIAL DEPLOYMENT ANGLE. (DEG) POSITIVE DOWNWARD
C
C*************************************************************************
C
C  ADDITIONAL INPUT NEEDED FOR IOPT = 1 ONLY
C
C          AMO   -  STEADY-STATE MOUTH AREA. (FT2)
C          ASO   -  CANOPY DESIGN SURFACE AREA. (FT2)
C            K   -  CLOTH PERMEABILITY CONSTANT
C           CP   -  PRESSURE COEFFICIENT
C            N   -  CLOTH PERMEABILITY EXPONENT
C           VO   -  GEOMETRIC VOLUME. (FT3)
C
C*************************************************************************
C
      REAL*4 N
      TODEN=100000.
    5 PRINT *,'INPUT IOPT'
      READ(5,*,END=100) IOPT
      PRINT *,'INPUT ALT,RHO,VS,CDSO,TO,W,J,TAU,ALPHA(0)'
      READ(5,*),ALT,RHO,VS,CDSO,TO,W,J,TAU,ALPHA0
      IF(IOPT.EQ.2) GO TO 3
      PRINT *,'INPUT AMO,ASO,K,CP,N,VO'
      READ(5,*) AMO,ASO,XK,CP,N,VO
    3 DT=TO/TODEN
      G=32.2
      S=0.
      X=TAU
```

TABLE 1. PARACHUTE PROGRAM (CONT.)

```
      CDS=TAU*CDSO
      FS=.5*RHO*VS**2*CDSO
      F=TAU*FS
      VOL=0.
      IPASS=0
      DT=10.*DT
      IF(IOPT.EQ.2) GO TO 8
    7 V=VS
      ALPHA=ALPHAO
      VOL=0.
      T=0.
      XM=(2.*W)/(RHO*G*CDSO*VS*TO)
    6 TFAC=(1.-TAU)*(T/TO)**J + TAU
      DVX=-V**2*COSD(ALPHA)*TFAC/(XM*VS*TO)*DT
      DVY=(G-V**2/(XM*VS*TO)*TFAC*SIND(ALPHA))*DT
      VX=V*COSD(ALPHA)
      VY=V*SIND(ALPHA)
      VX=VX+DVX
      VY=VY+DVY
      V=SQRT(VX**2+VY**2)
      DVOL=(V*AMO*(T/TO)**J-ASO*(T/TO)**J*XK*(CP*RHO/2.)**N
     1 *V**(2.*N))*DT
      VOL=VOL+DVOL
      IF(VX.NE.0.) ALPHA=ATAND(VY/VX)
      T=T+DT
      IF(T.GE.TO) GO TO 4
      GO TO 6
    4 IF(VOL.GT.(VO-10.) .AND. VOL.LT.(VO+10.)) GO TO 8
      TO=TO*(VO/VOL)
      IF(IPASS.GT.50) STOP 'VOLUME ITERATION FAILED AFTER 50 PASSES'
      IPASS=IPASS+1
      GO TO 7
    8 CONTINUE
      XM=(2.*W)/(RHO*G*CDSO*VS*TO)
      T=0.
      V=VS
      ALPHA=ALPHAO
      R=0.
      S=0.
      DS=0.
      DPRINT=TO/50.
      DT=DT/10.
      WRITE(6,10)
   10 FORMAT(1H1'DEPLOYMENT CONDITIONS',17X,'SYSTEM PARAMETERS')
      WRITE(6,11) ALT,CDSO
   11 FORMAT(1HO,3X,'ALTITUDE =',F7.0,' FT',15X,'STEADY STATE DRAG AREA'
     1' CDSO =',F8.2,' FT2')
      WRITE(6,12) RHO,W
   12 FORMAT(1H ,4X,'DENSITY =',F10.7,' SLUGS/FT3',24X,'WEIGHT W = ',
     1 F6.1,' LBS')
      WRITE(6,13) VS,TO
   13 FORMAT(1H ,'VELOCITY VS =',F6.1,' FT/SEC',22X,'INFLATION TIME TO =
     1', F7.3,' SEC')
      WRITE(6,14) J,FS
   14 FORMAT(1H ,10X,'J =',I2,24X,'STEADY STATE DRAG FROCE FS =',F9.1,
     1' LBS' )
      WRITE(6,15) TAU,XM
   15 FORMAT(1H ,8X,'TAU =',F6.3,45X,'M =',F8.5)
      WRITE(6,16) ALPHAO
   16 FORMAT(1H ,5X,'ALPHAO =',F6.2,' DEG')
      IF(IOPT.EQ.1) WRITE(6,19) N
```

TABLE 1. PARACHUTE PROGRAM (CONT.)

```
   19 FORMAT(1H+, 64X, 'N =', F6.3)
      IF(IOPT.EQ.1) WRITE(6,17) AMO, ASO, XK, VO, CP
   17 FORMAT(62X, 'AMO =', F8.2, ' FT2'/
     1       62X, 'ASO =', F8.2, ' FT2'/
     2       64X, 'K =', F6.2/
     3       58X, 'VO GEOM =', F9.2, ' FT3'/
     4       61X, 'C.P. =' F6.2)
      WRITE(6,18)
   18 FORMAT(1H0)
      WRITE(6,20)
   20 FORMAT(2X, 'TIME', 3X, 'VELOCITY', 4X, 'ALPHA', 4X, 'RANGE', 7X, 'S',
     1 6X, 'DISTANCE', 6X, 'SHOCK', 9X, 'F'/
     2 3X, 'SEC', 4X, 'FT/SEC', 6X, 'DEG', 7X, 'FT', 8X, 'FT', 8X, 'FT', 8X,
     3 'FACTOR', 8X, 'LBS')
      LCOUNT=11
      F=0.
      IBYPASS=0
      IF(IOPT.EQ.1) LCOUNT=16
C
C  IBYPASS=0  FORCE HAS NOT REACHED A MAXIMUM, CONTINUE CALCULATION.
C  IBYPASS=1  FORCE HAS REACHED A MAXIMUM, STOP CALCULATION IF T>TO.
C
   35 IF(T/TO.GT.1.001  AND.IBYPASS.NE.0) GO TO 5
      IF(LCOUNT.LT.54) GO TO 38
      WRITE(6,37)
   37 FORMAT(1H1)
      WRITE(6,20)
      LCOUNT=3
   38 LCOUNT=LCOUNT+1
      WRITE(6,30) T, V, ALPHA, R, S, DS, X, F
   30 FORMAT(1X, F5.3, F10.2, F10.2, F9.1, 2F11.2, 1PE13.3, 0PF11.1)
      TOLD=T+DPRINT
      IF(DT.GT.DPRINT) TOLD=T+DT
   40 TPREV=T
      T=T+DT
      IF(T.GT.TOLD) T=TOLD
      TOVTO=(1.-TAU)*(T/TO)**J + TAU
      CDS=CDSO*TOVTO
      DVX=-V**2*COSD(ALPHA)*TOVTO/(XM*VS*TO)*DT
      DVY=(G-V**2*TOVTO*SIND(ALPHA)/(XM*VS*TO))*DT
      VX=V*COSD(ALPHA)
      VY=V*SIND(ALPHA)
      VX=VX+DVX
      VY=VY+DVY
      V=SQRT(VX**2+VY**2)
      IF(VX.NE.0.) ALPHA=ATAND(VY/VX)
      R=R+VX*DT
      S=S+VY*DT
      DS=DS+V*DT
      X=(V/VS)**2*CDS/CDSO
      FOLD=F
      F=X*FS
      IF(IBYPASS.EQ.1) GO TO 99
      IF(T-TPREV.LT.DT) GO TO 99
      IF(F.GE.FOLD) GO TO 99
      IBYPASS=1
      WRITE(6,98) T, V, ALPHA, R, S, DS, X, F
   98 FORMAT(1X, F5.3, F10.2, F10.2, F9.1, 2F11.2, 1PE13.3, 0PF11.1,
     1 ' MAX FORCE')
      LCOUNT=LCOUNT+1
   99 IF(T.LT.TOLD) GO TO 40
      GO TO 35
  100 STOP
      END
```

TABLE 2. GENERAL TRAJECTORY TECHNIQUE MODE 1 COMPUTER SOLUTION OF EXAMPLE 1: TOWARD-THE-EARTH-DELIVERY CONDITION, $\gamma = 90^\circ$

DEPLOYMENT CONDITIONS

ALTITUDE = 3000. FT
DENSITY = 0.0021753 SLUGS/FT3
VELOCITY VS = 325.3 FT/SEC
J = 6
TAU = 0.000
ALPHAO = 90.00 DEG

SYSTEM PARAMETERS

STEADY-STATE DRAG AREA CDSO = 725.58 FT2
WEIGHT W = 200.0 LBS
INFLATION TIME TO = 0.751 SEC.
STEADY-STATE DRAG FROCE FS = 83485.1 LBS
M = 0.03221
N = 0.500
AMO = 399.53 FT2
ASO = 962.10 FT2
K = 1.46
VO GEOM = 4690.83 FT3
C.P. = 1.70

TIME SEC	VELOCITY FT/SEC	ALPHA DEG	RANGE FT	S FT	DISTANCE FT	SHOCK FACTOR	F LBS	
0.000	325.25	90.00	0.0	0.00	0.00	0.000E+00	0.0	
0.015	325.71	90.00	0.0	4.89	4.89	6.418E-11	0.0	
0.030	326.17	90.00	0.0	9.79	9.79	4.119E-09	0.0	
0.045	326.63	90.00	0.0	14.70	14.70	4.705E-08	0.0	
0.060	327.08	90.00	0.0	19.61	19.61	2.651E-07	0.0	
0.075	327.54	90.00	0.0	24.53	24.53	1.014E-06	0.1	
0.090	328.00	90.00	0.0	29.46	29.46	3.037E-06	0.3	
0.105	328.46	90.00	0.0	34.39	34.39	7.679E-06	0.6	
0.120	328.92	90.00	0.0	39.33	39.33	1.716E-05	1.4	
0.135	329.38	90.00	0.0	44.28	44.28	3.488E-05	2.9	
0.150	329.84	90.00	0.0	49.23	49.23	6.562E-05	5.5	
0.165	330.30	90.00	0.0	54.19	54.19	1.169E-04	9.8	
0.180	330.75	90.00	0.0	59.16	59.16	1.976E-04	16.5	
0.195	331.19	90.00	0.0	64.13	64.13	3.203E-04	26.7	
0.210	331.59	90.00	0.0	69.12	69.12	5.009E-04	41.8	
0.225	331.95	90.00	0.0	74.10	74.10	7.593E-04	63.4	
0.240	332.24	90.00	0.0	79.09	79.09	1.120E-03	93.5	
0.255	332.45	90.00	0.0	84.09	84.09	1.614E-03	134.7	
0.270	332.55	90.00	0.0	89.08	89.08	2.276E-03	190.0	
0.286	332.49	90.00	0.0	94.08	94.08	3.146E-03	262.7	
0.301	332.23	90.00	0.0	99.07	99.07	4.274E-03	356.8	
0.316	331.71	90.00	0.0	104.06	104.06	5.709E-03	476.6	
0.331	330.86	90.00	0.0	109.04	109.04	7.509E-03	626.9	
0.346	329.61	90.00	0.0	114.01	114.01	9.730E-03	812.3	
0.361	327.87	90.00	0.0	118.95	118.95	1.243E-02	1037.6	
0.376	325.52	90.00	0.0	123.86	123.86	1.565E-02	1306.7	
0.391	322.47	90.00	0.0	128.73	128.73	1.943E-02	1622.5	
0.406	318.60	90.00	0.0	133.55	133.55	2.379E-02	1986.2	
0.421	313.79	90.00	0.0	138.30	138.30	2.871E-02	2396.5	
0.436	307.94	90.00	0.0	142.98	142.98	3.412E-02	2848.9	
0.451	300.94	90.00	0.0	147.55	147.55	3.994E-02	3334.6	
0.466	292.75	90.00	0.0	152.02	152.02	4.601E-02	3841.5	
0.481	283.31	90.00	0.0	156.35	156.35	5.214E-02	4353.0	
0.496	272.66	90.00	0.0	160.53	160.53	5.808E-02	4849.2	
0.511	260.84	90.00	0.0	164.54	164.54	6.359E-02	5308.6	
0.526	247.98	90.00	0.0	168.36	168.36	6.839E-02	5709.4	
0.541	234.24	90.00	0.0	171.99	171.99	7.226E-02	6032.2	
0.556	219.82	90.00	0.0	175.40	175.40	7.501E-02	6262.0	
0.571	204.98	90.00	0.0	178.59	178.59	7.653E-02	6389.5	
0.581	194.93	90.00	0.0	180.60	180.60	7.686E-02	6416.5	MAX FORCE
0.586	189.95	90.00	0.0	181.56	181.56	7.681E-02	6412.6	
0.601	174.99	90.00	0.0	184.30	184.30	7.588E-02	6335.1	
0.616	160.33	90.00	0.0	186.82	186.82	7.387E-02	6167.3	
0.631	146.17	90.00	0.0	189.12	189.12	7.095E-02	5923.4	
0.646	132.68	90.00	0.0	191.22	191.22	6.732E-02	5620.2	
0.661	119.97	90.00	0.0	193.12	193.12	6.318E-02	5274.9	
0.676	108.13	90.00	0.0	194.83	194.83	5.874E-02	4904.0	
0.691	97.21	90.00	0.0	196.37	196.37	5.416E-02	4522.0	
0.706	87.21	90.00	0.0	197.76	197.76	4.960E-02	4141.0	
0.721	78.13	90.00	0.0	199.00	199.00	4.516E-02	3770.5	
0.736	69.92	90.00	0.0	200.11	200.11	4.093E-02	3417.4	
0.751	62.54	90.00	0.0	201.10	201.10	3.697E-02	3086.3	

volume is not within specified limits, the program adjusts "t_o" by equation (11) and reiterates the program until the calculated volume is within the specified limits. The geometric volume of the parachute is determined using the methods of Section VIII of Appendix A.

$$t_o = t_o \frac{V_{o\ geometric}}{V_{o\ calc.}} \qquad (11)$$

Mode 2 of the program calculates opening shock profiles for input values of t_o. Mode 2 analysis of other types of parachutes is possible by the selection of the proper values of "j" (1/2, 1, 2, 3, 4, 5, or 6) and "τ". In most applications τ may be assumed to be zero.

When a given system is deployed at the same altitude and velocity, but at various trajectory angles, the inflation reference time is a maximum for the vertical away-from-the-earth trajectory and a minimum for the vertical toward-the-earth trajectory. The inflation reference times and opening shock forces vary accordingly with trajectory deployment angle between these limits. As the altitude increases the variation of opening shock force with trajectory angle is minimized.

Equation (10) is the identical expression as used in Reference 2 for the vertical toward-the-earth mode of delivery. The velocity term of equation (10) is the only element not associated with the parachute geometry or canopy cloth airflow. The inflation time is determined by the trajectory velocity variation, and the velocity variation depends on the trajectory deployment angle.

This method is best suited to the solid-cloth family of parachutes. It does, however, give a choice of methods for horizontal deployments. Reference 1 assumes that the trajectory remains horizontal throughout the inflation process and provides a convenient closed form method of calculating opening shock force which does not require the use of a computer. This method requires a computer, but does include the two-dimensional trajectory space variation.

EXAMPLES OF APPLICATION

As a demonstration of the method, a solid-cloth parachute of 35 feet D_o diameter and 30 gores is to be used to retard a 200-pound weight. Determine the effects of trajectory deployment angle, altitude, and cloth rate of airflow on the inflation time and opening shock force when deployed at constant velocity and constant dynamic pressure.

1. Parachute geometry

a. Parachute surface area:

$$S_o = \frac{\pi}{4} D_o^2$$

$$S_o = \frac{\pi}{4} (35)^2$$

$$S_o = 962.1 \text{ ft}^2$$

b. Parachute drag area: Preliminary design C_D=0.75

$$C_D S_o = 0.75 \times 962.1$$

$$C_D S_o = 721.6 \text{ ft}^2$$

From Table 2, page A-15 of Appendix A, the following inflated shape data were obtained for a 30-gore solid-cloth flat circular parachute. See Figure 24 of Appendix A for shape nomenclature.

$$\frac{2\bar{a}}{D_o} = 0.668; \frac{N}{\bar{a}} = 0.827; \frac{b}{\bar{a}} = 0.6214; \frac{b'}{\bar{a}} = 0.7806$$

c. Steady-state inflated canopy radius:

$$\bar{a} = \frac{.668\, D_o}{2}$$

$$\bar{a} = \frac{0.668 \times 35}{2}$$

$$\bar{a} = 11.69 \text{ ft.}$$

d. Steady-state mouth area:

$$A_{Mo} = \pi \bar{a}^2 \left[1 - \left(\frac{N/\bar{a} - b/\bar{a}}{b'/\bar{a}}\right)^2\right]$$

$$A_{Mo} = \pi (11.69)^2 \left[1 - \left(\frac{0.827 - 0.6214}{0.7806}\right)^2\right]$$

$$A_{Mo} = 399.53 \text{ ft}^2$$

e. Steady-state canopy volume of air to be collected, V_o geometric.

$$V_o = \frac{2}{3}\pi\bar{a}^3\left[\frac{b}{\bar{a}} + \frac{b'}{\bar{a}}\right]$$

$$V_o = \frac{2}{3}\pi(11.69)^3\left[0.6214 + 0.7807\right]$$

$$V_o = 4690.83\ ft^3$$

The program of Table 1 was initiated to determine the inflation reference time and opening shock force profiles for the example 1 parachute system deployed at various trajectory angles from vertical away-from-the-earth (-90^o) to vertical toward-the-earth ($+90^o$) at increments of 15 degrees. The analysis is conducted at altitudes of sea level, 3,000, and 20,000 feet. At each altitude the effects of a constant velocity of 325.25 fps and a constant dynamic pressure of 125.7 psf are examined. Cloth airflow variations are illustrated by assigning the cloth airflow exponent "n" (equation 10) values of 0.5 and 0.632. The assumption of n=0.5 allows a closed form solution for t_o in Reference 1. The n=0.632 is a measured value for the cloth of the illustrative parachute. The results of example 1 are presented in Figures 2 through 5, and Tables 2 and 3.

For any given altitude at constant velocity the maximum inflation reference time, Figure 2, minimum opening shock force, Figure 3, and minimum time of occurrence in the inflation process, Table 3, occur in the vertical trajectory away from the earth. Conversely, the minimum inflation reference time, maximum opening shock force and maximum time of occurrence in the inflation process occur in the vertical trajectory toward-the-earth. When the value of the cloth airflow parameter,n, is varied from 0.5 to 0.632, the inflation reference times are extended with a subsequent reduction of the maximum opening shock forces and time of occurrence of the maximum force at all trajectory angles.

As the altitude increases, the inflation reference time decreases, Figure 2; the maximum shock force increases, Figure 3; and the maximum force occurs later in the inflation process, Table 3.

When a constant dynamic pressure analysis profile is substituted for the constant velocity profile the effects of trajectory angle, n, and deployment altitude show the same trends but different magnitudes than the constant velocity approach. See Figures 4 and 5 and Table 3. At sea level the constant velocity and constant dynamic pressure results are identical. At all other altitudes the parachute opens faster with an increase in opening shock force.

The variation of opening shock force as a function of trajectory launch angle tends to equalize as the altitude increases. Table 4 illustrates the force variation for the

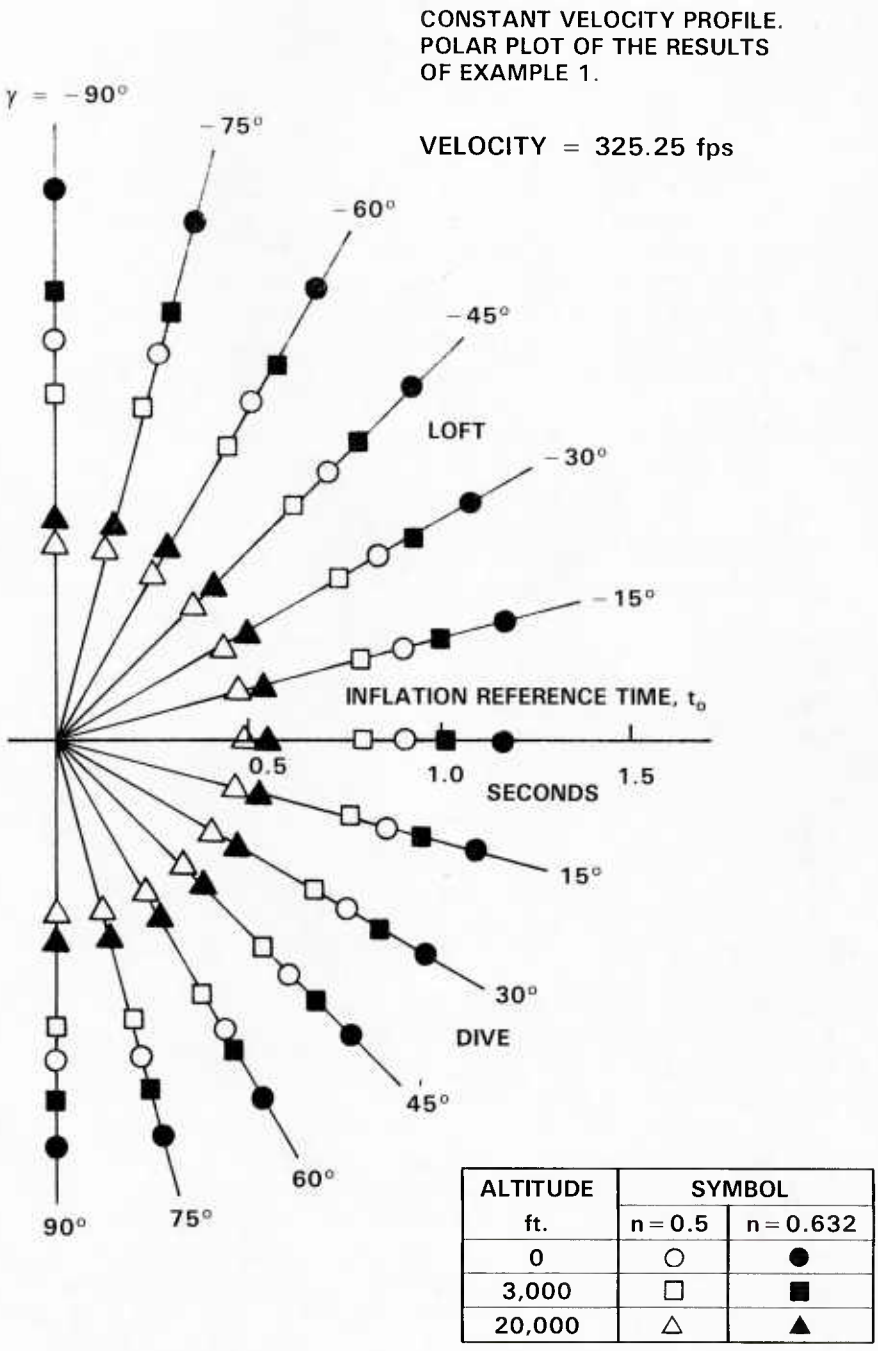

ALTITUDE	SYMBOL	
ft.	n = 0.5	n = 0.632
0	○	●
3,000	□	■
20,000	△	▲

ALTITUDE	γ (deg)	n = 0.500 t_o (sec)	n = 0.662 t_o (sec)
SEA LEVEL	−90	1.054	1.416
	−75	1.047	1.401
	−60	1.026	1.362
	−45	0.998	1.311
	−30	0.970	1.259
	−15	0.940	1.213
	0	0.913	1.171
	15	0.894	1.138
	30	0.874	1.108
	45	0.860	1.088
	60	0.849	1.074
	75	0.841	1.065
	90	0.839	1.062
3,000 ft	−90	0.904	1.171
	−75	0.900	1.163
	−60	0.894	1.142
	−45	0.876	1.111
	−30	0.854	1.079
	−15	0.833	1.046
	0	0.813	1.018
	15	0.794	0.992
	30	0.779	0.972
	45	0.767	0.955
	60	0.758	0.944
	75	0.753	0.938
	90	0.751	0.936
20,000 ft	−90	0.513	0.590
	−75	0.512	0.589
	−60	0.509	0.585
	−45	0.504	0.579
	−30	0.499	0.572
	−15	0.493	0.565
	0	0.486	0.559
	15	0.481	0.551
	30	0.476	0.545
	45	0.471	0.539
	60	0.469	0.537
	75	0.467	0.534
	90	0.466	0.534

FIGURE 2. EFFECTS OF TRAJECTORY LAUNCH ANGLE, ALTITUDE, AND CLOTH RATE OF AIRFLOW ON THE PARACHUTE INFLATION REFERENCE TIME AT CONSTANT VELOCITY, EXAMPLE 1

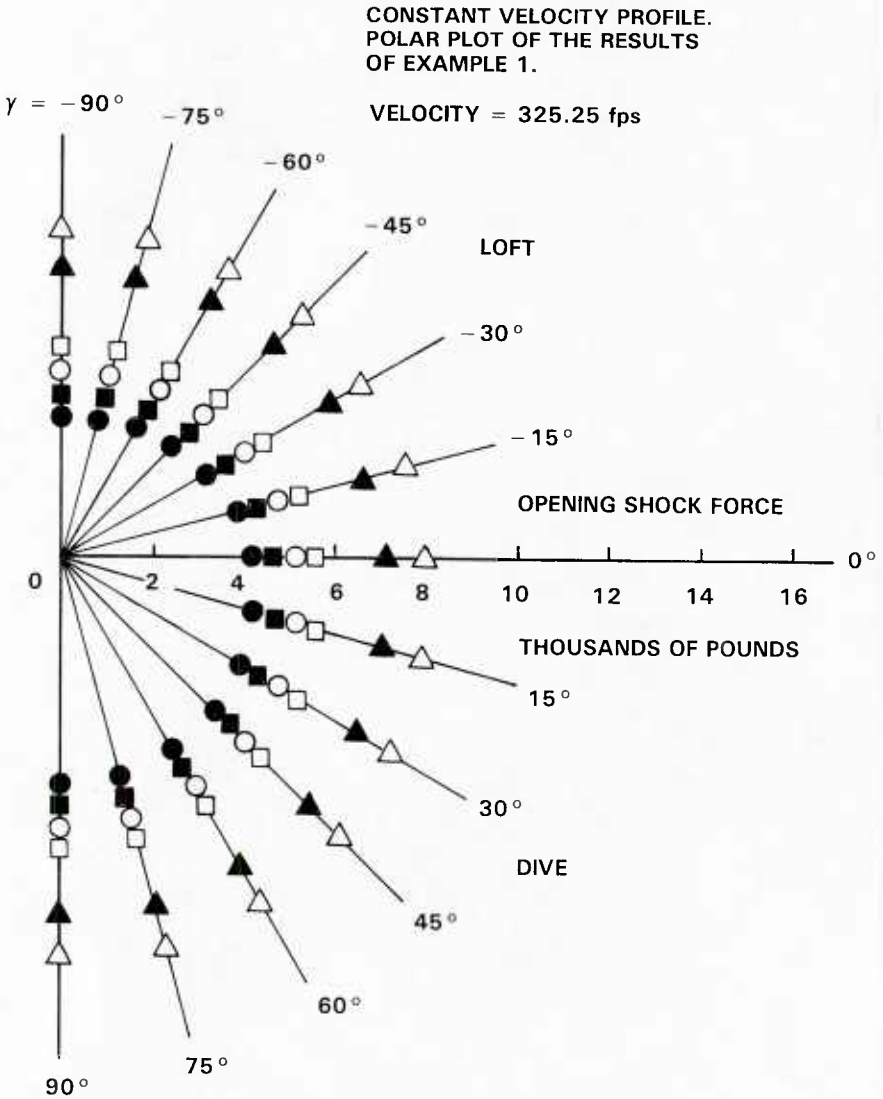

ALTITUDE	SYMBOL	
ft.	n = 0.5	n = 0.632
0	○	●
3,000	□	■
20,000	△	▲

ALTITUDE	γ (deg)	n = 0.500 F_{MAX} (lbs)	n = 0.662 F_{MAX} (lbs)
SEA LEVEL	−90	4024.6	3017.2
	−75	4077.6	3075.1
	−60	4200.2	3210.3
	−45	4393.9	3414.5
	−30	4613.3	3647.8
	−15	4868.7	3897.5
	0	5122.3	4139.0
	15	5336.6	4370.8
	30	5542.8	4571.9
	45	5716.6	4737.6
	60	5836.9	4850.5
	75	5933.4	4932.2
	90	5949.1	4947.7
3,000 ft	−90	4594.3	3584.5
	−75	4637.4	3634.7
	−60	4709.7	3743.7
	−45	4885.6	3926.8
	−30	5097.0	4134.7
	−15	5337.6	4378.0
	0	5567.5	4600.5
	15	5817.0	4833.4
	30	6015.8	5020.8
	45	6192.5	5191.5
	60	6310.6	5302.1
	75	6398.5	5381.9
	90	6416.5	5395.8
20,000 ft	−90	7143.9	6288.7
	−75	7186.9	6327.8
	−60	7271.7	6408.1
	−45	7416.5	6547.4
	−30	7582.9	6718.1
	−15	7792.3	6917.9
	0	7996.7	7102.5
	15	8205.1	7323.4
	30	8384.1	7491.0
	45	8549.7	7657.4
	60	8644.0	7755.2
	75	8743.2	7833.7
	90	8756.4	7845.1

FIGURE 3. EFFECTS OF TRAJECTORY LAUNCH ANGLE, ALTITUDE, AND CLOTH RATE OF AIRFLOW ON THE MAXIMUM OPENING SHOCK FORCE AT CONSTANT VELOCITY, EXAMPLE 1

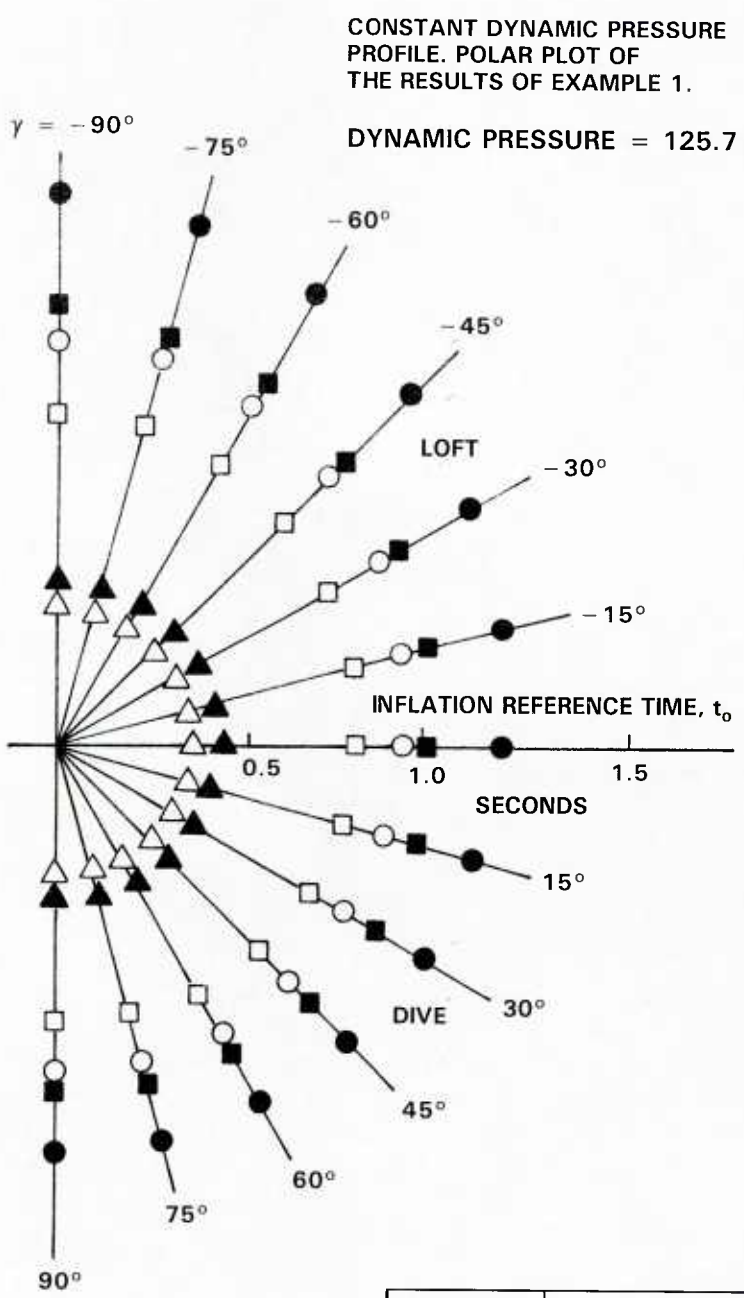

ALTITUDE	SYMBOL	
ft.	n = 0.5	n = 0.632
0	○	●
3,000	□	■
20,000	△	▲

ALTITUDE	γ (deg)	n = 0.500 t_o (sec)	n = 0.662 t_o (sec)
SEA LEVEL	−90	1.054	1.418
	−75	1.048	1.400
	−60	1.027	1.363
	−45	0.999	1.312
	−30	0.968	1.260
	−15	0.941	1.214
	0	0.913	1.172
	15	0.894	1.138
	30	0.874	1.109
	45	0.860	1.089
	60	0.850	1.074
	75	0.842	1.066
	90	0.840	1.063
3,000 ft	−90	0.862	1.115
	−75	0.859	1.109
	−60	0.849	1.090
	−45	0.834	1.065
	−30	0.814	1.036
	−15	0.795	1.008
	0	0.778	0.982
	15	0.762	0.958
	30	0.749	0.941
	45	0.738	0.925
	60	0.730	0.916
	75	0.725	0.909
	90	0.724	0.908
20,000 ft	−90	0.366	0.433
	−75	0.365	0.433
	−60	0.364	0.432
	−45	0.362	0.429
	−30	0.361	0.428
	−15	0.358	0.425
	0	0.357	0.422
	15	0.354	0.419
	30	0.352	0.416
	45	0.350	0.414
	60	0.349	0.412
	75	0.348	0.411
	90	0.348	0.411

FIGURE 4. EFFECTS OF TRAJECTORY LAUNCH ANGLE, ALTITUDE, AND CLOTH RATE OF AIRFLOW ON THE PARACHUTE INFLATION REFERENCE TIME AT CONSTANT DYNAMIC PRESSURE, EXAMPLE 1

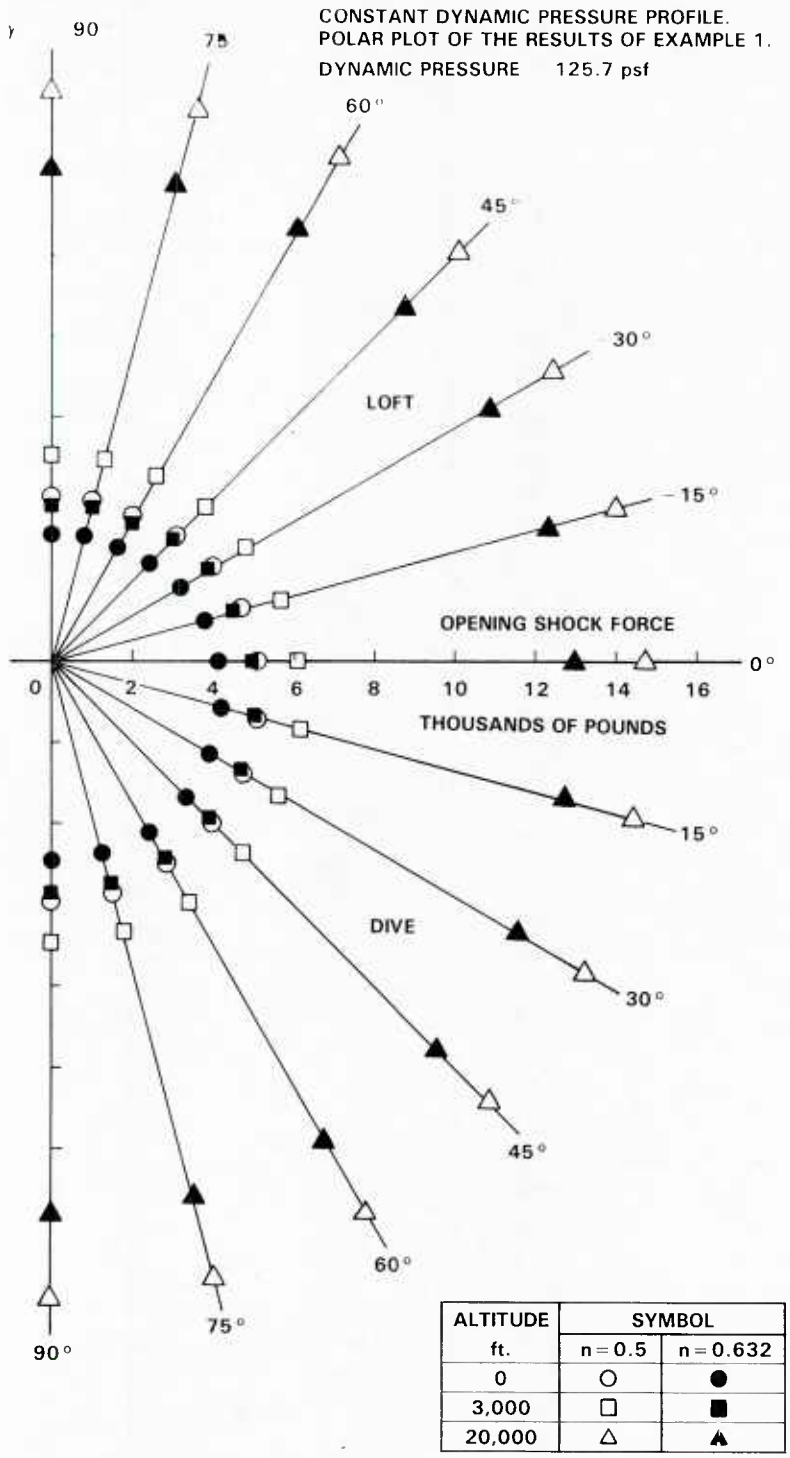

ALTITUDE ft.	SYMBOL n = 0.5	SYMBOL n = 0.632
0	○	●
3,000	□	■
20,000	△	▲

ALTITUDE	γ (deg)	n = 0.500 F_{MAX} (lbs)	n = 0.632 F_{MAX} (lbs)
SEA LEVEL	−90	4018.8	3011.3
	−75	4070.6	3075.9
	−60	4194.1	3205.7
	−45	4386.6	3409.0
	−30	4616.0	3642.8
	−15	4861.7	3892.4
	0	5106.8	4132.5
	15	5329.5	4365.4
	30	5536.3	4566.1
	45	5709.0	4732.0
	60	5829.6	4843.7
	75	5925.4	4926.4
	90	5942.3	4942.8
3,000 ft	−90	5075.1	3977.6
	−75	5121.9	4027.2
	−60	5224.0	4139.7
	−45	5392.9	4312.3
	−30	5609.8	4525.3
	−15	5852.3	4760.5
	0	6085.3	4989.9
	15	6325.9	5227.3
	30	6525.2	5412.8
	45	6704.1	5584.7
	60	6825.4	5692.2
	75	6913.2	5779.1
	90	6929.2	5792.4
20,000 ft	−90	14091.6	12133.3
	−75	14161.1	12174.7
	−60	14242.8	12249.6
	−45	14373.1	12385.1
	−30	14516.0	12526.6
	−15	14748.8	12722.6
	0	14916.4	12919.1
	15	15143.2	13134.9
	30	15328.8	13313.6
	45	15489.1	13473.9
	60	15608.2	13582.9
	75	15696.7	13664.7
	90	15699.6	13679.6

FIGURE 5. EFFECTS OF TRAJECTORY LAUNCH ANGLE, ALTITUDE, AND CLOTH RATE OF AIRFLOW ON THE MAXIMUM OPENING SHOCK FORCE AT CONSTANT DYNAMIC PRESSURE, EXAMPLE 1

TABLE 3. EFFECTS OF TRAJECTORY LAUNCH ANGLE, ALTITUDE, AND CLOTH RATE OF AIRFLOW ON THE TIME OF OCCURRENCE OF THE MAXIMUM SHOCK FORCE DURING THE INFLATION PROCESS

ALTITUDE	γ (DEG)	CONSTANT VELOCITY n = 0.500 t/t_o @F_{max}	CONSTANT VELOCITY n = 0.632 t/t_o @F_{max}	CONSTANT DYNAMIC PRESSURE n = 0.500 t/t_o @F_{max}	CONSTANT DYNAMIC PRESSURE n = 0.632 t/t_o @F_{max}
SEA LEVEL	-90	.7296	.6995	0.7296	0.6989
	-75	.7307	.7002	0.7309	0.7000
	-60	.7329	.7034	0.7332	0.7029
	-45	.7355	.7071	0.7357	0.7073
	-30	.7371	.7109	0.7386	0.7103
	-15	.7415	.7139	0.7407	0.7142
	0	.7442	.7182	0.7437	0.7167
	15	.7461	.7188	0.7461	0.7197
	30	.7471	.7229	0.7483	0.7223
	45	.7477	.7233	0.7500	0.7236
	60	.7503	.7244	0.7494	0.7244
	75	.7515	.7249	0.7506	0.7251
	90	.7521	.7269	0.7512	0.7262
3,000 FT.	-90	.7555	.7260	0.7564	0.7283
	-75	.7556	.7274	0.7555	0.7286
	-60	.7573	.7312	0.7562	0.7303
	-45	.7591	.7336	0.7590	0.7333
	-30	.7611	.7359	0.7617	0.7355
	-15	.7647	.7400	0.7635	0.7381
	0	.7663	.7417	0.7661	0.7403
	15	.7683	.7450	0.7677	0.7432
	30	.7702	.7459	0.7690	0.7439
	45	.7718	.7476	0.7696	0.7459
	60	.7731	.7479	0.7712	0.7467
	75	.7729	.7495	0.7724	0.7481
	90	.7736	.7500	.7721	0.7478
20,000 FT.	-90	.8850	.8678	0.8880	0.8684
	-75	.8848	.8676	0.8877	0.8661
	-60	.8861	.8684	0.8874	0.8657
	-45	.8869	.8705	0.8895	0.8695
	-30	.8878	.8724	0.8892	0.8668
	-15	.8884	.8726	0.8911	0.8682
	0	.8930	.8730	0.8908	0.8697
	15	.8919	.8748	0.8927	0.8687
	30	.8929	.8771	0.8920	0.8702
	45	.8960	.8776	0.8943	0.8720
	60	.8955	.8771	0.8940	0.8714
	75	.8951	.8783	0.8937	0.8735
	90	.8948	.8783	0.8937	0.8710

TABLE 4. EFFECTS OF ALTITUDE AND CANOPY CLOTH RATE OF AIR FLOW ON THE RATIO OF THE MAXIMUM OPENING SHOCK FORCE OF THE VERTICAL TOWARD-THE-EARTH, AND VERTICAL AWAY-FROM-THE-EARTH TRAJECTORIES AT CONSTANT VELOCITY AND DYNAMIC PRESSURE

	$R = \frac{F_{max} @ \gamma = 90^{o}}{F_{max} @ \gamma = -90^{o}}$			
ALTITUDE (ft.)	CONSTANT VELOCITY V = 325.25 fps		CONSTANT DYNAMIC PRESSURE q = 125.7 psf	
	n = 0.5	n = 0.632	n = 0.5	n = 0.632
0	1.48	1.64	1.48	1.64
3K	1.40	1.51	1.37	1.46
20K	1.23	1.25	1.11	1.13
50K	1.16	1.17	1.021	1.022
100K	1.155	1.157	1.0012	1.0016

toward-the-earth and the away-from-the-earth trajectories as affected by altitude and the rate of cloth airflow, n.

$$R = \frac{F_{max} @ \gamma = 90^{\circ}}{F_{max} @ \gamma = -90^{\circ}} \qquad (12)$$

As the altitude continues to increase, the force ratio R approaches one indicating that at some altitude the opening shock force is essentially independent of the trajectory deployment angle. Note that the effect of the value of n is converging. Figure 6 shows that at high altitudes the inflation reference time is basically no longer a function of n or k. The air density is a factor affecting the rate of flow through the canopy surface. As the density approaches zero the mass flow ratio, M', approaches zero. See Section VII of Appendix A for a discussion of Mass Flow Ratio. Figures 7 through 11 illustrate the effects of cloth airflow rate on the inflation reference time, inflation distance and opening shock force as a function of altitude for the parameters of example 1.

COMPARISON OF OPENING SHOCK FORCES CALCULATED BY THE METHODS OF REFERENCE 1 AND THE GENERAL TRAJECTORY TECHNIQUE

The opening shock force comparisons are limited to a trajectory deployment angle of $\gamma = 0^{o}$. The horizontal trajectory deployment reference time is calculated via equation (14A) from page A-7 of Appendix A.

$$t_o = \frac{2W}{\rho g V_s C_D S_o}\left[e^{\frac{g\rho V_o}{2W}\left[\frac{C_D S_o}{A_{Mo} - A_{so}\, k\left(\frac{C_p\,\rho}{2}\right)^{1/2}}\right]_{-1}}\right] \qquad (14A)$$

In equation (14A) τ was assumed to be zero and n was assigned the value of 0.500.

The MIL-C-7020, type III canopy cloth airflow constant is k=1.46 and the average pressure coefficient is taken to be $C_p' = 1.7$. For a sea level velocity of 325.25 fps.

$$t_o = \frac{14 \times 200}{0.002378 \times 32.2 \times 325.25 \times 721.58}\left[e^{K1} - 1\right]$$

$$K1 = \frac{32.2 \times 0.002378 \times 4690.83}{2 \times 200}\left[\frac{721.58}{399.53 - 962.1\,(1.46)\left(\frac{0.002378 \times 1.7}{2}\right)^{1/2}}\right]$$

$$t_o = 0.913 \text{ sec.}$$

The ballistic mass ratio for $t_o = 0.913$ sec.

$$M = \frac{2W}{\rho g V_s t_o C_D S_o}$$

$$M = \frac{2 \times 200}{0.002378 \times 32.2 \times 325.25 \times 0.913 \times 721.58}$$

$$M = 0.0244$$

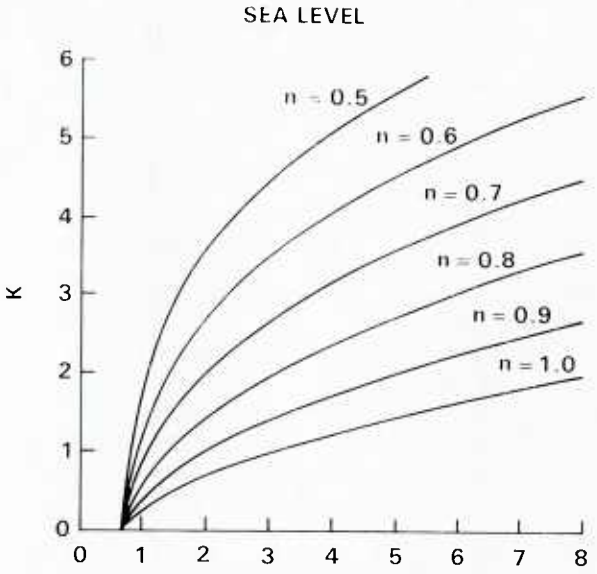

A. INFLATION REFERENCE TIME (SEC)

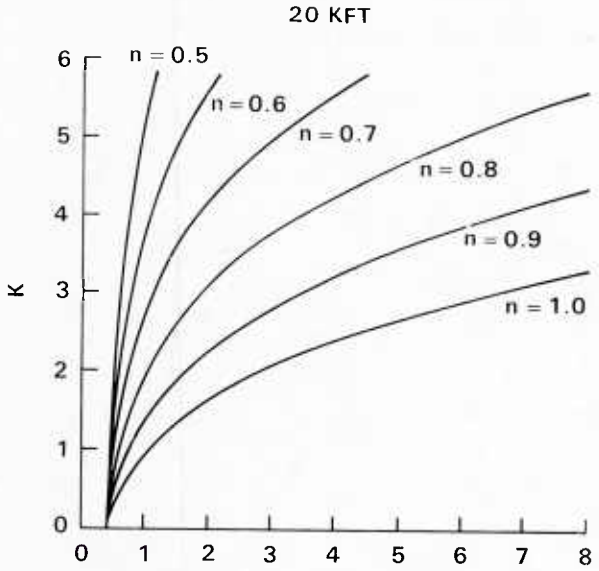

B. INFLATION REFERENCE TIME (SEC)

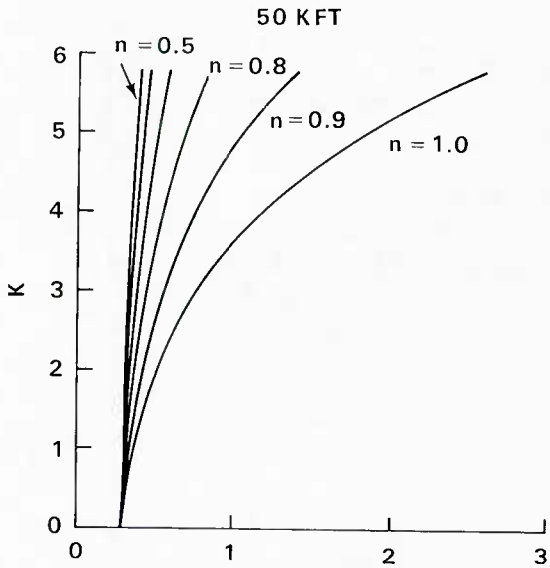

C. INFLATION REFERENCE TIME (SEC)

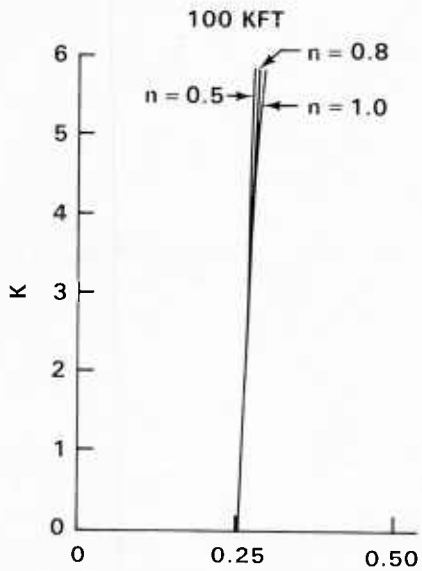

D. INFLATION REFERENCE TIME (SEC)

CLOTH	k	n
MIL-C-7020, TYPE III	1.46042	0.63246
MIL-C-8021, TYPE I	0.99469	0.57403
MIL-C-8021, TYPE II	0.44117	0.60492

FIGURE 6. EFFECT OF CANOPY CLOTH CONSTANTS "k" and "n" ON THE PARACHUTE INFLATION REFERENCE TIME "T_o"

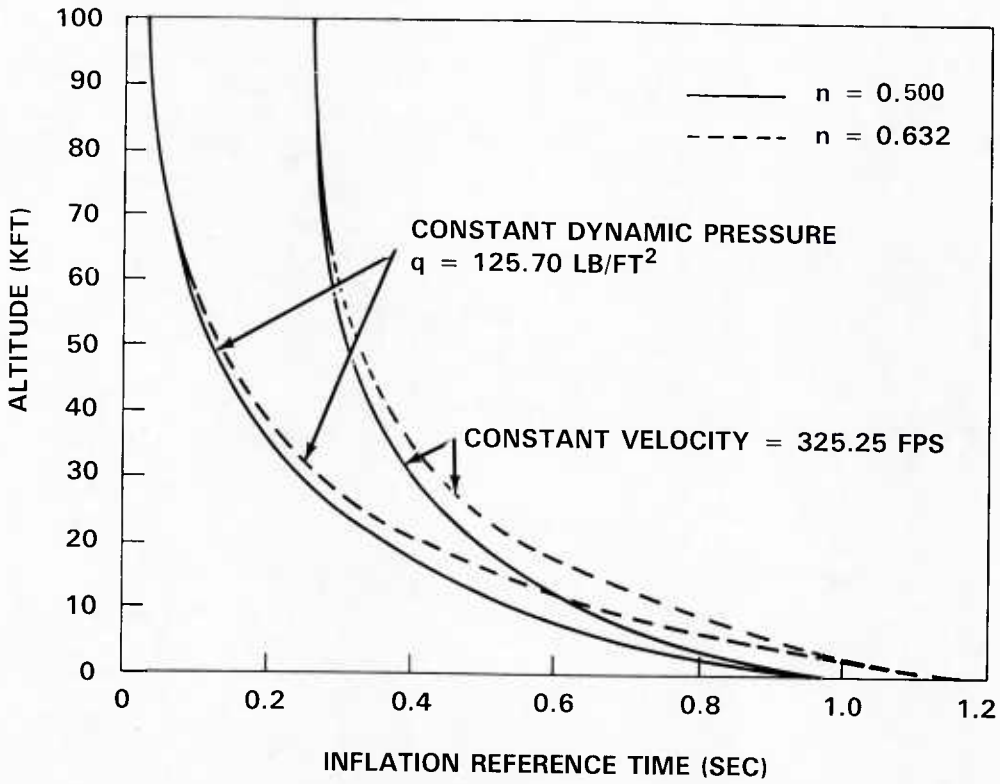

FIGURE 7. EFFECT OF ALTITUDE ON THE INFLATION REFERENCE TIME "T_o"

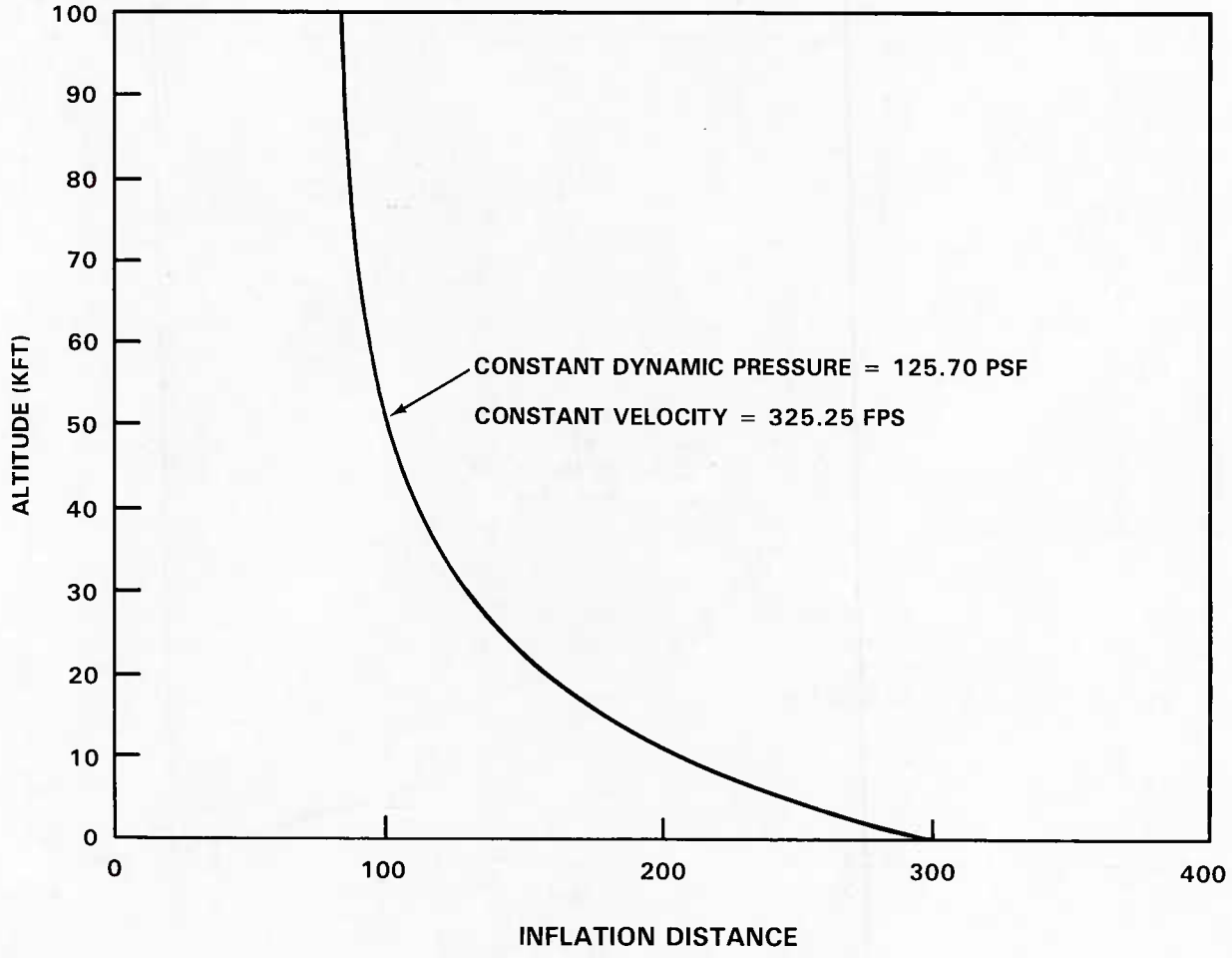

FIGURE 8. EFFECT OF ALTITUDE ON THE INFLATION DISTANCE (FEET)
$n = 0.500, \gamma = 0^{\circ}, \tau = 0$

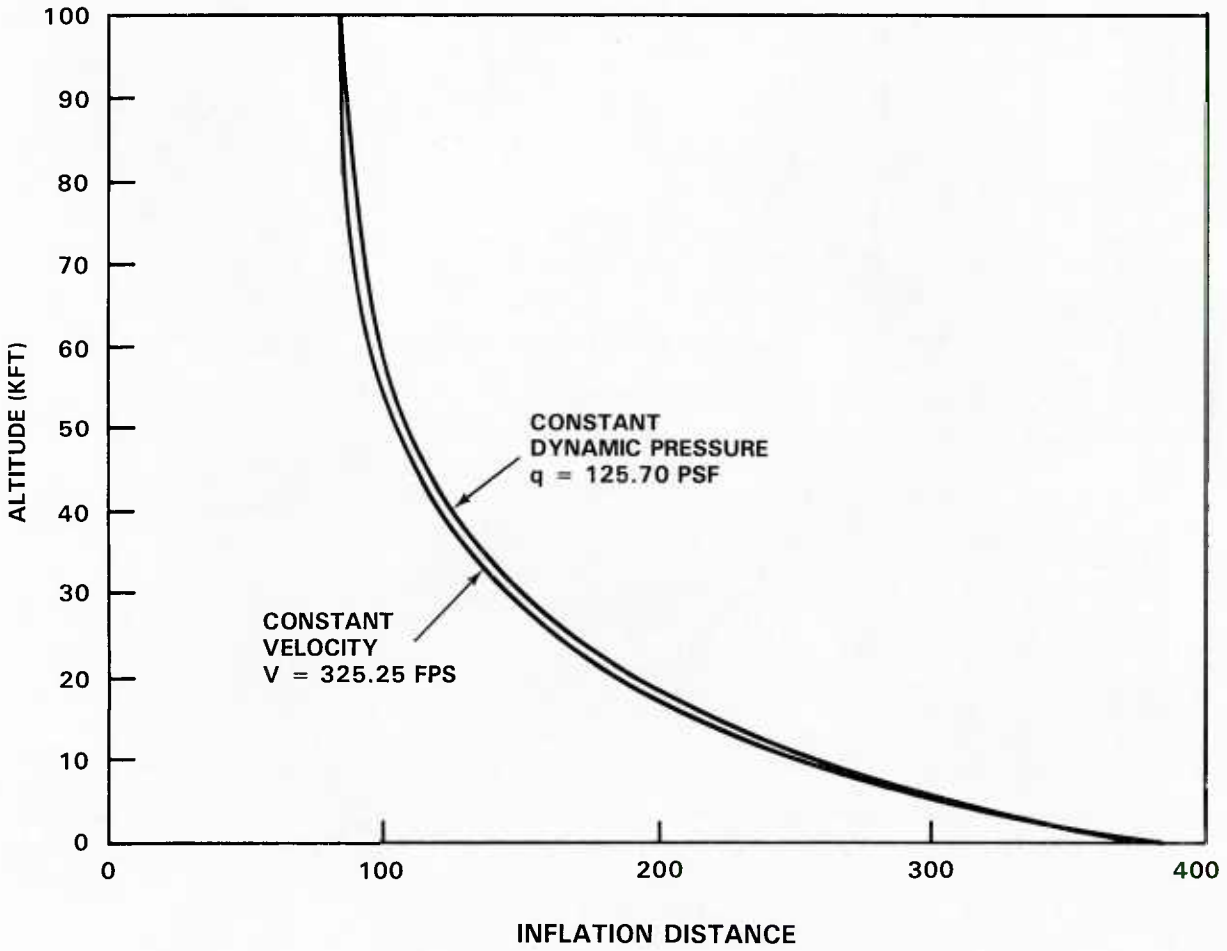

FIGURE 9. EFFECT OF ALTITUDE ON THE INFLATION DISTANCE (FEET)
n = 0.632, $\gamma = 0^{\circ}$, $\tau = 0$

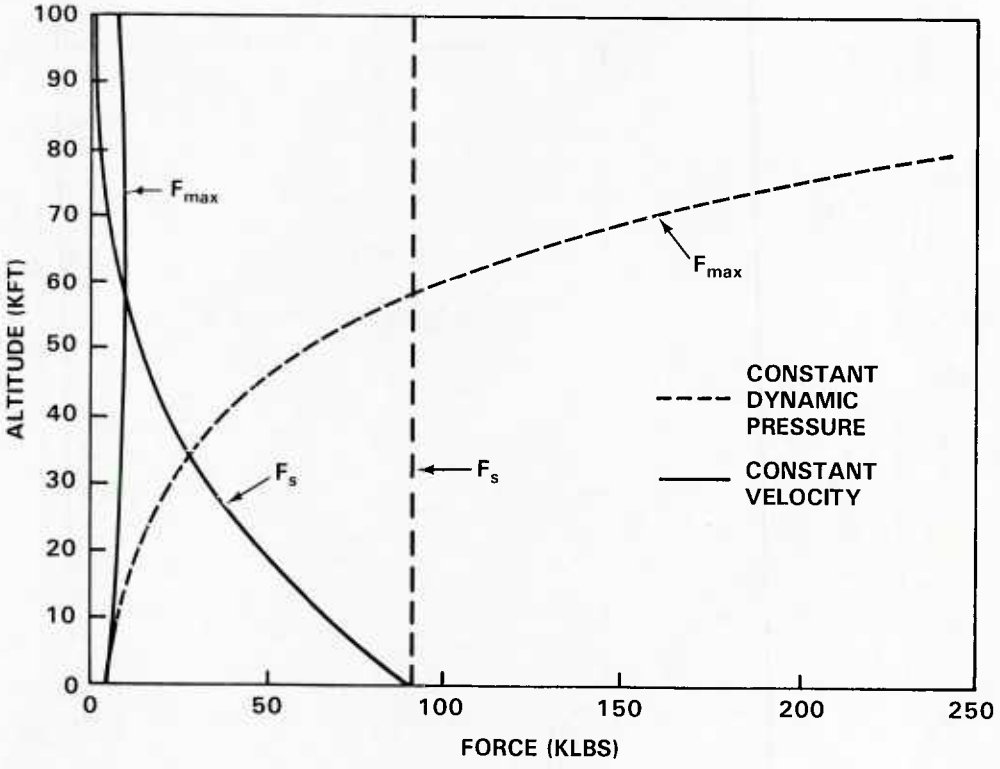

FIGURE 10. VARIATION OF STEADY-STATE DRAG AND MAXIMUM OPENING SHOCK FORCE WITH ALTITUDE FOR n = 0.500, $\gamma = 0^{\circ}$, $\tau = 0$

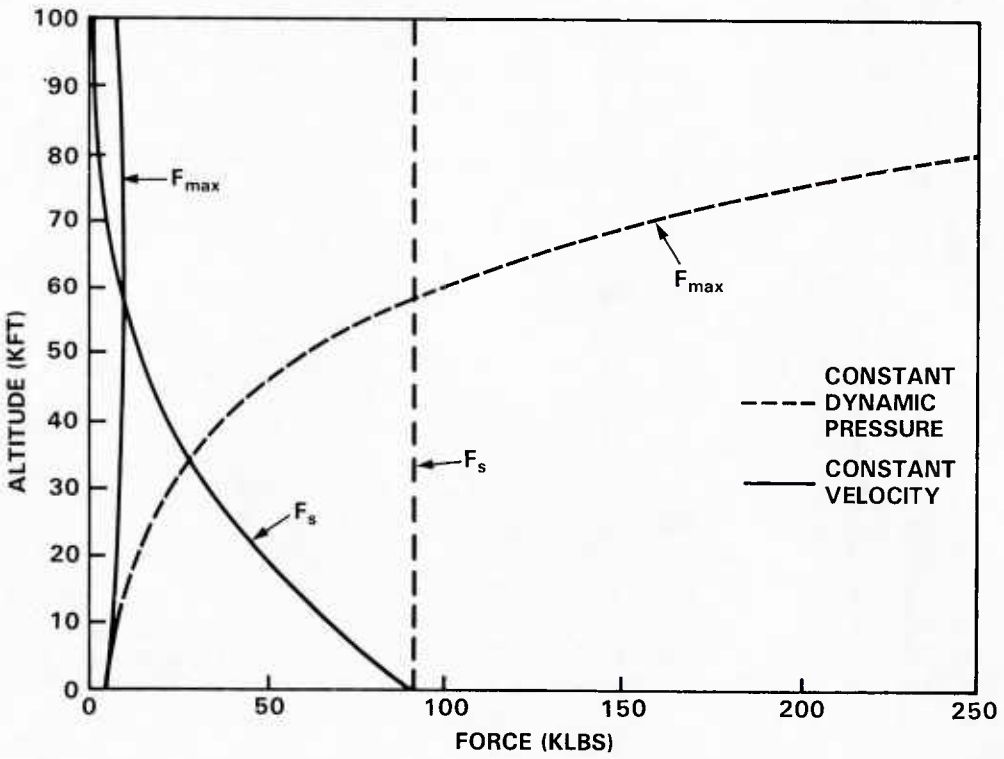

FIGURE 11. VARIATION OF STEADY-STATE DRAG AND MAXIMUM OPENING SHOCK FORCE WITH ALTITUDE FOR n = 0.632, $\gamma = 0^{\circ}$, $\tau = 0$

Since the ballistic mass ratio is less than the limiting value of $M_L = 0.1907$, the inflation performance is in the finite mass range of operation and $t_o = t_f$. The following formulae were obtained from Table 12 of Reference 1 for values of j=6 and τ=0.

The time of occurrence of the maximum shock force during canopy inflation:

$$\frac{t}{t_o} @ \chi_{i_{max}} = \left(\frac{21M}{4}\right)^{1/7}$$

$$\frac{t}{t_o} @ \chi_{i_{max}} = \left(\frac{21 \times 0.0244}{4}\right)^{1/7}$$

$$\frac{t}{t_o} @ \chi_{i_{max}} = 0.7454$$

The maximum shock factor:

$$\chi_{i_{max}} = \frac{16}{49}\left(\frac{21M}{4}\right)^{6/7}$$

$$\chi_{i_{max}} = \frac{16}{49}\left(\frac{21 \times 0.0244}{4}\right)^{6/7}$$

$$\chi_{i_{max}} = 0.0560$$

The steady-state drag force:

$$F_s = \frac{1}{2}\rho V_s^2 C_D S_o$$

$$F_s = \frac{1}{2} \times 0.002378\ (340)^2\ 721.6$$

$$F_s = 90761.4 \text{ lb.}$$

The maximum shock force in the horizontal mode of deployment:

$$F_{max} = \chi_{i_{max}} F_s$$

$$F_{max} = 0.0560 \times 90761.4$$

$$F_{max} = 5082.6$$

TABLE 5. COMPARISON OF OPENING SHOCK FORCES CALCULATED FROM THE METHOD OF REFERENCE 1 AND THE GENERAL TRAJECTORY TECHNIQUE $\gamma = 0°, n = 0.500, \tau = 0$

		METHOD OF REFERENCE 1						RATIO
	ATL Kft	t_o sec.	M	t/t_o @ χ_{imax}	χ_{imax}	F_s lb.	F_{max} lb.	GTT / REF. 1
CONSTANT VELOCITY	0	0.914	0.024	0.745	0.0560	90,761.4	5,082.6	1.0078
	3	0.808	0.030	0.768	0.0672	83,058.4	5,581.5	0.9975
	20	0.485	0.086	0.893	0.1655	48,390.3	8,008.6	0.9985
CONSTANT "q"	0	0.914	0.024	0.745	0.0560	90,761.4	5,082.6	1.0048
	3	0.773	0.030	0.768	0.0672	90,761.4	6,099.2	0.9977
	20	0.354	0.086	0.893	0.1655	90,761.4	15,021.0	0.9930
		GENERAL TRAJECTORY TECHNIQUE (GTT)						
CONSTANT VELOCITY	0	0.913	0.024	0.744	0.0554	90,761.4	5,122.3	
	3	0.813	0.029	0.766	0.0660	83,058.4	5,567.5	
	20	0.486	0.086	0.893	0.1656	48,390.3	7,996.7	
CONSTANT q	0	0.913	0.024	0.744	0.0554	90,761.4	5,106.8	
	3	0.778	0.029	0.766	0.0660	90,761.4	6,085.3	
	20	0.357	0.086	0.891	0.1656	90,761.4	14,916.4	

A series of opening shock force calculations were conducted for constant velocity and constant dynamic pressure profiles for trajectory deployment angles of $\gamma = 0^{\circ}$ at sea level and altitudes of 3,000 feet and 20,000 feet. The results are summarized in Table 5. An examination of Table 5 indicates that the forces calculated by the method of Reference 1 and the general trajectory technique agree within less than $\pm$ 1%, and therefore the methods are consistent and interchangeable.

DISCUSSION OF SYSTEM PERFORMANCE

The listed performance of method 1 shows the same values for M, t/t_o @ $x_{i\ max}$, and x_{imax} for constant velocity and constant dynamic pressure at a designated altitude. Yet the inflation reference times and opening shock forces vary. How this occurs is as follows:

Two major design considerations for any parachute system are the required rate of descent (V_e) and the altitude at which it is to be achieved.

$$\frac{W}{C_D S_o} = \frac{1}{2} \rho V_e^2$$

Once these decisions are firm the system, $W/C_D S_O$ has been established. The particular system weight to be recovered defines the parachute aerodynamic size ($C_D S_O$). The geometric size (D_O) and inflated shape and volume are a result of the type of parachute and canopy rate of airflow selected.

Multiplying both sides of equation (14A) by V_s shows that the inflation distance is dependent on the parachute geometry, cloth airflow properties, $W/C_D S_O$, and altitude.

$$V_s t_o = \frac{2W}{\rho g\, C_D S_o} \left[e^{\frac{g\rho V_o}{2W} \left[\frac{C_D S_o}{A_{Mo} - A_{so}\, k \left(\frac{C_p \rho}{2} \right)^{1/2}} \right]} - 1 \right]$$

When the parachute type, canopy cloth, and suspension line length have been selected, the only variable undefined is the operational altitude. The inflation distance does not depend on the operational velocity, but the inflation reference time does. Rather, the inflation distance has been preordained by the system requirements, size, and operational altitude.

The inflation distance is used to determine the BMR which is also not a function of velocity, but does depend on the operational altitude.

$$M = \frac{2W}{\rho g V_s t_o C_D S_o}$$

The time of occurrence of the maximum shock factor during the inflation process, and the maximum shock factor are defined by the BMR.

$$\frac{t}{t_o} @ \lambda_{i_{max}} = \left(\frac{21M}{4}\right)^{1/7}$$

$$\lambda_{i_{max}} = \frac{16}{49}\left(\frac{21M}{4}\right)^{6/7}$$

The conclusion to be drawn from this is that the entire performance of the parachute system was defined by the initial decisions of rate of descent, altitude at which the rate of descent is required, system weight, parachute type, canopy cloth, and parachute geometry including suspension line length. The performance varies with operational altitude.

The BMR is the scale parameter which determines what percentage of the steady-state drag force, F_s, is to be realized as opening shock force. As the operational density altitude is raised the inflation distance is reduced and the resulting BMR is raised. Selecting a constant velocity-altitude profile determines the locus of the variation of the steady-state drag force. A constant dynamic pressure locus of variation is another convenient way of determining how the required line stretch velocity varies with altitude for the purpose of providing a basis for analysis and comparison. However, the percentage of the steady-state drag destined to become opening shock force is the same for both profiles for a given altitude.

EXAMPLE 2 - Compare the opening shock forces of a ribbon parachute retardation system using the methods of Reference 1 and the general trajectory technique.

a. Altitude = 3,000 ft. ; ρ = 0.0021752 slugs per ft^3.

b. System weight = 4,000 lb.

c. Parachute diameter = 35 ft; S_o = 962.1 ft^2

d. Trajectory velocity = 340 fps

e. Trajectory angle $\gamma = 0^o$

f. Initial drag area $\tau = 0$

g. j=1

Parachute inflation time:

$$t_o = \frac{nD_o}{V_s}$$

where n=14 for ribbon parachutes

$$t_o = \frac{14 \times 35}{340}$$

$$t_o = 1.441 \text{ sec.}$$

The parachute drag area:

$$C_D S_o = 0.5 \times 962.1$$

$$C_D S_o = 481 \text{ ft}^2$$

The ballistic mass ratio:

$$M = \frac{2W}{\rho g V_s t_o C_D S_o}$$

$$M = \frac{2 \times 4000}{0.0021753 \times 32.2 \times 340 \times 1.441 \times 481.0}$$

$$M = 0.4847$$

The time of occurrence in the deployment process:

$$\chi_{i_{max}} = \left(\frac{9}{16}\right)\left(\frac{2M}{3}\right)^{1/2}$$

$$\chi_{i_{max}} = \left(\frac{9}{16}\right)\left(\frac{2 \times 0.4847}{3}\right)^{1/2}$$

$$\chi_{i_{max}} = 0.3197$$

The maximum shock factor:

$$\frac{t}{t_o} @ \chi_{i_{max}} = \left(\frac{2M}{3}\right)^{1/2}$$

$$\frac{t}{t_o} @ \chi_{i_{max}} = \left(\frac{2 \times 0.4847}{3}\right)^{1/2}$$

$$\frac{t}{t_o} @ \chi_{i_{max}} = 0.5684$$

The steady state drag force:

$$F_s = \frac{1}{2} \rho V_s^2 C_D S_o$$

$$F_s = \frac{1}{2} \times 0.0021753 (340)^2 481.0$$

$$F_s = 60{,}474.5 \text{ lb.}$$

The maximum shock force:

$$F_{max} = \chi_{i_{max}} F_s$$

$$F_{max} = 0.3197 \times 60{,}474.5$$

$$F_{max} = 19{,}333.7 \text{ lb.}$$

The computer solution of example 2 is presented in Table 6 and a comparison of the results with the method of Reference 1 is shown in Table 7.

TABLE 6. GENERAL TRAJECTORY TECHNIQUE MODE 2 COMPUTER SOLUTION OF EXAMPLE 2

DEPLOYMENT CONDITIONS

ALTITUDE 3000 FT
DENSITY 0.0021752 SLUGS/FT^3
VELOCITY VS 340.0 FT/SEC
J 1
TAU 0.000
ALPHAO 0.00 DEG

SYSTEM PARAMETERS

STEADY-STATE DRAG AREA' CDSO = 481.00 FT^2
WEIGHT W = 4000.0 LBS
INFLATION TIME TO = 1.441 SEC
STEADY-STATE DRAG FORCE FS = 60474.5 LBS
M = 0.48460

TIME SEC	VELOCITY FT/SEC	ALPHA DEG	RANGE FT	S FT	DISTANCE FT	SHOCK FACTOR	F LBS	
0.000	340.00	0.00	0.0	0.00	0.00	0.000E+00	0.0	
0.029	339.86	0.16	9.8	0.01	9.80	1.998E-02	1208.5	
0.058	339.44	0.31	19.6	0.05	19.59	3.987E-02	2411.1	
0.086	338.75	0.47	29.4	0.12	29.37	5.956E-02	3601.9	
0.115	337.79	0.63	39.1	0.21	39.13	7.896E-02	4775.2	
0.144	336.56	0.79	48.9	0.33	48.85	9.798E-02	5925.6	
0.173	335.06	0.94	58.5	0.48	58.54	1.165E-01	7047.7	
0.202	333.32	1.10	68.2	0.65	68.18	1.345E-01	8136.8	
0.231	331.32	1.26	77.8	0.85	77.76	1.519E-01	9188.4	
0.259	329.10	1.42	87.3	1.07	87.28	1.686E-01	10198.4	
0.288	326.64	1.59	96.7	1.32	96.73	1.846E-01	11163.3	
0.317	323.97	1.75	106.1	1.59	106.10	1.997E-01	12079.7	
0.346	321.10	1.91	115.4	1.89	115.39	2.141E-01	12945.2	
0.375	318.04	2.08	124.6	2.21	124.60	2.275E-01	13757.6	
0.404	314.79	2.25	133.7	2.56	133.71	2.400E-01	14515.2	
0.432	311.38	2.42	142.7	2.92	142.73	2.515E-01	15216.8	
0.461	307.82	2.59	151.6	3.31	151.65	2.623E-01	15862.0	
0.490	304.12	2.76	160.4	3.72	160.47	2.720E-01	16450.5	
0.519	300.29	2.94	169.1	4.16	169.18	2.808E-01	16982.2	
0.548	296.34	3.12	177.7	4.61	177.77	2.887E-01	17457.5	
0.576	292.30	3.30	186.2	5.09	186.25	2.956E-01	17878.0	
0.605	288.16	3.48	194.5	5.58	194.61	3.017E-01	18244.6	
0.634	283.95	3.67	202.7	6.09	202.85	3.069E-01	18559.3	
0.663	279.68	3.85	210.8	6.63	210.97	3.113E-01	18823.2	
0.692	275.35	4.05	218.8	7.18	218.97	3.148E-01	19038.0	
0.721	270.98	4.24	226.7	7.74	226.84	3.176E-01	19207.0	
0.749	266.59	4.44	234.4	8.33	234.58	3.197E-01	19332.6	
0.778	262.17	4.64	242.0	8.93	242.20	3.211E-01	19417.2	
0.807	257.72	4.84	249.4	9.55	249.69	3.218E-01	19458.4	
0.823	255.23	4.96	253.6	9.91	253.84	3.219E-01	19467.5	MAX FORCE
0.836	253.30	5.05	256.8	10.19	257.05	3.219E-01	19467.3	
0.865	248.88	5.26	264.0	10.84	264.28	3.215E-01	19442.4	
0.894	244.47	5.47	271.0	11.50	271.39	3.205E-01	19384.1	
0.922	240.08	5.69	278.0	12.18	278.37	3.191E-01	19297.0	
0.951	235.71	5.91	284.8	12.87	285.22	3.172E-01	19182.9	
0.980	231.38	6.14	291.5	13.58	291.95	3.149E-01	19044.3	
1.009	227.08	6.37	298.1	14.30	298.55	3.123E-01	18883.3	
1.038	222.83	6.61	304.5	15.03	305.03	3.093E-01	18702.4	
1.066	218.63	6.85	310.8	15.77	311.39	3.060E-01	18503.7	
1.095	214.48	7.09	317.0	16.53	317.63	3.024E-01	18289.2	
1.124	210.38	7.34	323.1	17.30	323.75	2.986E-01	18060.4	
1.153	206.34	7.59	329.0	18.08	329.76	2.947E-01	17819.3	
1.182	202.37	7.85	334.9	18.87	335.64	2.905E-01	17567.8	
1.211	198.46	8.11	340.6	19.67	341.42	2.862E-01	17307.4	
1.239	194.61	8.38	346.2	20.48	347.08	2.818E-01	17039.4	
1.268	190.83	8.65	351.7	21.31	352.63	2.772E-01	16765.1	
1.297	187.12	8.93	357.1	22.14	358.07	2.726E-01	16486.1	
1.326	183.48	9.21	362.3	22.98	363.41	2.679E-01	16203.1	
1.355	179.92	9.50	367.5	23.83	368.65	2.632E-01	15917.6	
1.384	176.42	9.79	372.6	24.69	373.78	2.585E-01	15630.5	
1.412	172.99	10.09	377.5	25.56	378.81	2.537E-01	15342.4	
1.441	169.64	10.40	382.4	26.44	383.75	2.489E-01	15054.0	

TABLE 7. COMPARISON OF THE RESULTS OF EXAMPLE 2

	$t/t_o @ \chi_{i_{max}}$	F_{max}
METHOD OF REFERENCE 1	0.5684	19,333.7
GENERAL TRAJECTORY TECHNIQUE	0.5711	19,467.5

The variation of the particular values determined by the two methods is less than one percent.

CONCLUSIONS

1. The comparison of the maximum opening shock forces computed by the methods of reference 1 and this report for trajectory deployment angles of zero degrees are in agreement by less than plus or minus one percent. The two methods are therefore consistent and interchangeable.

2. For a given system deployed under similar conditions of altitude and velocity the maximum opening shock force depends on the trajectory angle at parachute inflation. The minimum shock force occurs in the vertical, away-from-the-earth trajectory, and the maximum shock force occurs in the vertical, toward-the-earth trajectory. As altitude increases the ratio of the maximum opening shock force in the vertical toward-the-earth trajectory to the maximum opening shock force in the vertical away-from-the earth trajectory approaches one. The opening shock force at high altitudes is not as dependent on trajectory deployment angle as it is at low altitudes.

3. As the trajectory deployment angle varies from a climb to a dive attitude the maximum shock force varies from minimum to maximum.

4. At low altitudes the cloth airflow parameters k and n affect the canopy inflation characteristics. Extending the inflation distance results in a lowering of the maximum shock force. As the altitude increases, the effects of the variation of k and n on the inflation distance are minimized due to the air density reduction.

5. As the altitude increases the maximum shock force increases due to an increase in the BMR.

6. The weight-to-drag-area ratio is usually determined from the requirement for a given rate of descent at a given altitude. This ratio, the choice of parachute type, canopy cloth, and suspension line length define the inflation distance of the system for a given altitude. The inflation distance decreases as altitude increases. The inflation distance is independent of deployment velocity; however, the inflation reference time is dependent upon deployment velocity.

7. The BMR, which is dependent on the inflation distance and altitude is also independent of deployment velocity. The time of occurrence of the maximum shock force during deployment and the magnitude of the maximum shock factor are determined by the BMR, type of parachute (j), and the initial drag area (τ). The deployment performance is independent of deployment velocity.

8. The BMR determines what percentage of the steady-state drag force is to be realized as opening shock force in the particular deployment condition. Selection of a constant velocity or a constant dynamic pressure versus altitude profile determines the magnitude of the steady-state drag force which determines the opening shock force.

9. The program mode 1 method for solid-cloth parachutes can be expanded to other types of canopies when methods of describing the particular canopy outflow have been developed.

NOMENCLATURE

Symbols required for this report are listed on page A-16 of Appendix A. Additional symbols not listed in Appendix A are as follows:

j	Time ratio exponent used in the Pflanz and modified Pflanz drag area equations
N	Canopy depth of the inflated parachute
R	Ratio of the maximum opening shock force in the toward-the-earth trajectory to the opening shock force in the away-from-the-earth trajectory
V_e	Vertical rate descent, γ = 90 degrees, of the parachute system at the design altitude
γ	Trajectory angle to the horizontal at the time of parachute suspension line stretch. Loft trajectories are noted as negative angles. Dive angles are noted as positive angles
τ	Ratio of parachute drag area at t=0 to the steady-state drag area

REFERENCES

1. Ludtke, W.P., Notes On a Generic Parachute Opening Force Analysis, NSWC TR 86-142, March 1986

2. Ludtke, W.P., Notes On a Parachute Opening Force Analysis Applied to a Vertical Toward-The-Earth Trajectory, NSWC TR 87-96, May 1987

Appendix A

AIAA Paper No. 73-477

A TECHNIQUE FOR THE CALCULATION OF THE OPENING-SHOCK FORCES FOR SEVERAL TYPES OF SOLID CLOTH PARACHUTES

by
W. P. LUDTKE
Naval Ordnance Laboratory
Silver Spring, Maryland

AIAA 4th Aerodynamic Deceleration Systems Conference

PALM SPRINGS, CALIFORNIA / MAY 21-23, 1973

A TECHNIQUE FOR THE CALCULATION OF THE OPENING-SHOCK FORCES FOR SEVERAL TYPES OF SOLID CLOTH PARACHUTES

W. P. Ludtke
Naval Ordnance Laboratory
Silver Spring, Maryland

Abstract

An analytical method of calculating parachute opening-shock forces based upon wind-tunnel derived drag area time signatures of several solid cloth parachute types in conjunction with a scale factor and retardation system steady-state parameters has been developed. Methods of analyzing the inflation time, geometry, cloth airflow properties and materials elasticity are included. The effects of mass ratio and altitude on the magnitude and time of occurrence of the maximum opening shock are consistent with observed field test phenomena.

I. Introduction

In 1965, the Naval Ordnance Laboratory (NOL) was engaged in a project which utilized a 35-foot-diameter, 10-percent extended-skirt parachute (type T-10) as the second stage of a retardation system for a 250-pound payload. Deployment of the T-10 parachute was to be accomplished at an altitude of 100,000 feet. In this rarefied atmosphere, the problem was to determine the second stage deployment conditions for successful operation. A search of available field test information indicated a lack of data on the use of solid cloth parachutes at altitudes above 30,000 feet.

The approach to this problem was as follows: Utilizing existing wind-tunnel data, low-altitude field test data, and reasonable assumptions, a unique engineering approach to the inflation time and opening-shock problem was evolved that provided satisfactory results. Basically, the method combines a wind-tunnel derived drag area ratio signature as a function of deployment time with a scale factor and Newton's second law of motion to analyze the velocity and force profiles during deployment. The parachute deployment sequence is divided into two phases. The first phase, called "unfolding phase," where the canopy is undergoing changes in shape, is considered to be inelastic as the parachute inflates initially to its steady-state aerodynamic size for the first time. At this point, the "elastic phase" is entered where it is considered that the elasticity of the parachute materials enters the problem and resists the applied forces until the canopy has reached full inflation.

The developed equations are in agreement with the observed performance of solid cloth parachutes in the field, such as the decrease of inflation time as altitude increases, effects of altitude on opening-shock force, finite and infinite mass operation, and inflation distance.

II. Development of Velocity Ratio and Force Ratio Equations During the Unfolding Phase of Parachute Deployment

The parachute deployment would take place in a horizontal attitude in accordance with Newton's second law of motion.

$$\Sigma F = ma$$

$$-\frac{1}{2}\rho V^2 C_D S = \frac{W}{g}\frac{dV}{dt}$$

It was recognized that other factors, such as included air mass, apparent mass, and their derivatives, also contribute forces acting on the system. Since definition of these parameters was difficult, the analysis was conducted in the simplified form shown above. Comparison of calculated results and test results indicated that the omitted terms have a small effect.

$$\int_o^t C_D S dt = \frac{-2W}{\rho g}\int_{V_s}^{V}\frac{dV}{V^2} \qquad (1)$$

Multiplying the right-hand side of equation (1) by

$$1 = \frac{V_s t_o C_D S_o}{V_s t_o C_D S_o}$$

and rearranging

$$\frac{1}{t_o}\int_o^t \frac{C_D S}{C_D S_o}\, dt$$

$$= \frac{-2W}{\rho g V_s t_o C_D S_o} V_s \int_{V_s}^{V}\frac{dV}{V^2} \qquad (2)$$

In order to integrate the left-hand term of equation (2), the drag area ratio must be defined for the type of parachute under

analysis as a function of deployment reference time, t_o.

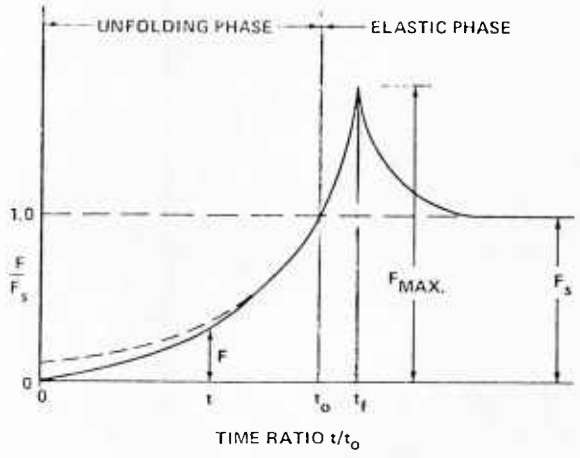

FIG. 1 TYPICAL INFINITE MASS FORCE-TIME HISTORY OF A SOLID CLOTH PARACHUTE IN A WIND TUNNEL

Figure 1 illustrates a typical solid cloth parachute wind-tunnel infinite mass force-time history after snatch. In infinite mass deployment, the maximum size and maximum shock force occur at the time of full inflation, t_f. However, t_f is inappropriate for analysis since it is dependent upon the applied load, structural strength, and materials elasticity. The reference time, t_o, where the parachute has attained its steady-state aerodynamic size for the first time, is used as the basis for performance calculations.

At any instant during the unfolding phase, the force ratio F/F_s can be determined as a function of the time ratio, t/t_o.

$$F = \frac{1}{2}\rho V^2 C_D S$$

$$F_s = \frac{1}{2}\rho V_s^2 C_D S_o$$

Since the wind-tunnel velocity and density are constant during infinite mass deployment

$$\frac{F}{F_s} = \frac{C_D S}{C_D S_o}$$

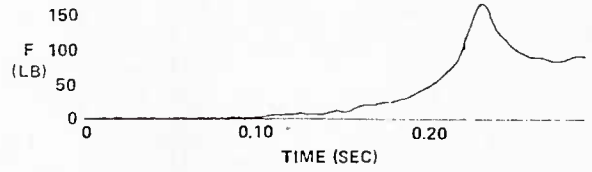

FIG. 2 TYPICAL FORCE-TIME CURVE FOR A SOLID FLAT PARACHUTE UNDER INFINITE MASS CONDITIONS.

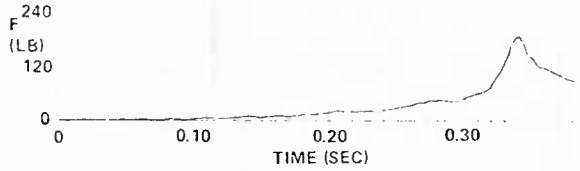

REPRODUCED FROM REFERENCE (1)

FIG. 3 TYPICAL FORCE-TIME CURVE FOR A 10% EXTENDED SKIRT PARACHUTE UNDER INFINITE MASS CONDITIONS.

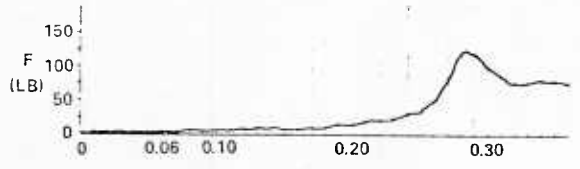

REPRODUCED FROM REFERENCE (1)

FIG. 4 TYPICAL FORCE-TIME CURVE FOR A PERSONNEL GUIDE SURFACE PARACHUTE UNDER INFINITE MASS CONDITIONS

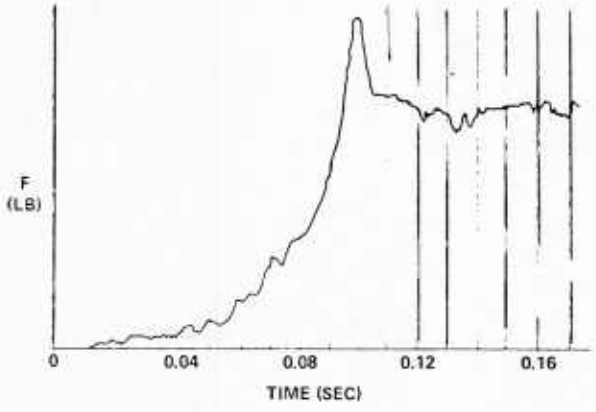

FIG. 5 TYPICAL FORCE-TIME SIGNATURE FOR THE ELLIPTICAL PARACHUTE UNDER INFINITE MASS CONDITIONS

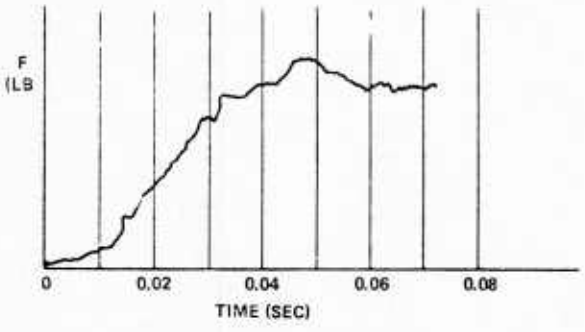

FIG. 6 TYPICAL FORCE-TIME SIGNATURE FOR THE RING SLOT PARACHUTE 20% GEOMETRIC POROSITY UNDER INFINITE MASS CONDITIONS

Infinite mass opening-shock signatures of several types of parachutes are presented in Figures 2 through 6. Analysis of these signatures using the force ratio, F/F_s, - time ratio, t/t_o, technique indicated a similarity in the performance of the various solid cloth types of

parachutes which were examined. The geometrically porous ring slot parachute displayed a completely different signature, as was expected. These data are illustrated in Figure 7. If an initial boundary

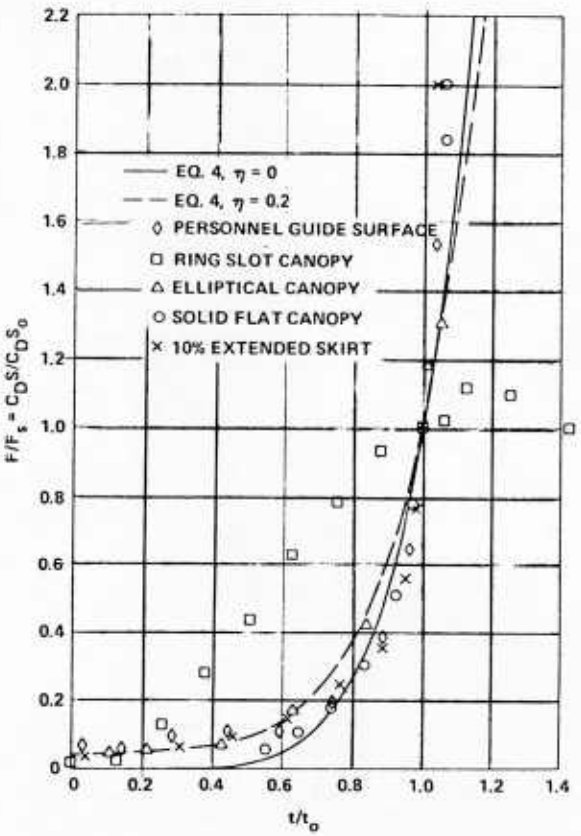

FIG. 7 DRAG AREA RATIO VS. TIME RATIO

condition of $C_DS/C_DS_o = 0$ at time $t/t_o = 0$ is assumed, then, the data can be approximated by fitting a curve of the form

$$\frac{C_DS}{C_DS_o} = \left(\frac{t}{t_o}\right)^6 \qquad (3)$$

A more realistic drag area ratio expression was determined which includes the effect of initial area at line stretch.

$$\frac{C_DS}{C_DS_o} = \left[\left(1-\eta\right)\left(\frac{t}{t_o}\right)^3 + \eta\right]^2 \qquad (4)$$

where η is the ratio of the projected mouth area at line stretch to the steady-state projected frontal area. Expanding equation (4)

$$\frac{C_DS}{C_DS_o} = \left(1-\eta\right)^2\left(\frac{t}{t_o}\right)^6 + 2\eta\left(1-\eta\right)\left(\frac{t}{t_o}\right)^3 + \eta^2 \qquad (5)$$

At the time that equation (5) was ascertained, it suggested that the geometry of the deploying parachute was independent of density and velocity. It was also postulated that although this expression had been determined for the infinite mass condition, it would also be true for the finite mass case. This phenomenon has since been independently observed and confirmed by Berndt and De Weese in reference (2).

Since the drag area ratio was determined from actual parachute deployments, it was assumed that the effects of apparent mass and included mass on the deployment force history were accommodated.

The right-hand term of equation (2) contains the expression

$$\frac{2W}{\rho g V_s t_o C_D S_o} = M \qquad (6)$$

This term can be visualized as shown in Figure 8 to be a ratio of the retarded mass (including the parachute) to an associated mass of atmosphere contained in a right circular cylinder which is generated by moving an inflated parachute of area C_DS_o for a distance equal to the product of V_st_o through an atmosphere of density, ρ.

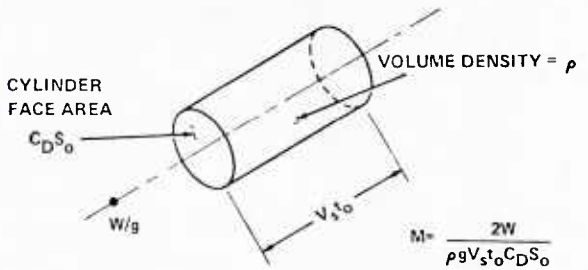

FIG. 8 VISUALIZATION OF THE MASS RATIO CONCEPT

The mass ratio, M, is the scale factor which controls the velocity and force profiles during parachute deployment. Substituting M and C_DS/C_DS_o into equation (2), integrating, and solving for V/V_s

$$\frac{V}{V_s} = \frac{1}{1+\frac{1}{M}\left[\frac{(1-\eta)^2}{7}\left(\frac{t}{t_o}\right)^7 + \frac{\eta(1-\eta)}{2}\left(\frac{t}{t_o}\right)^4 + \eta^2\frac{t}{t_o}\right]} \qquad (7)$$

The instantaneous shock factor is defined as

$$x_i = \frac{F}{F_s} = \frac{\frac{1}{2}\rho V^2 C_D S}{\frac{1}{2}\rho V_s^2 C_D S_o}$$

If the altitude variation during deployment is small, then, the density may be considered as constant

$$x_i = \frac{C_D S}{C_D S_o}\left(\frac{V}{V_s}\right)^2$$

from equations (5) and (7)

$$x_i = \frac{(1-\eta)^2\left(\frac{t}{t_o}\right)^6 + 2\eta(1-\eta)\left(\frac{t}{t_o}\right)^3 + \eta^2}{\left[1 + \frac{1}{M}\left[\frac{(1-\eta)^2}{7}\left(\frac{t}{t_o}\right)^7 + \frac{\eta(1-\eta)}{2}\left(\frac{t}{t_o}\right)^4 + \eta^2\frac{t}{t_o}\right]\right]^2} \quad (8)$$

III. Maximum Shock Force and Time of Occurrence During the Unfolding Phase

The time of occurrence of the maximum instantaneous shock factor, x_i, is difficult to determine for the general case. However, for $\eta = 0$, the maximum shock factor and time of occurrence are readily calculated. For $\eta = 0$

$$x_i = \frac{\left(\frac{t}{t_o}\right)^6}{\left[1 + \frac{1}{7M}\left(\frac{t}{t_o}\right)^7\right]^2}$$

Setting the derivative of x_i with respect to time equal to zero and solving for t/t_o at $x_{i\ max}$

$$\left(\frac{t}{t_o}\right)_{@\ x_{i\ max}} = \left(\frac{21M}{4}\right)^{\frac{1}{7}} \quad (9)$$

and the maximum shock factor is

$$x_{i\ max} = \frac{16}{49}\left(\frac{21M}{4}\right)^{\frac{6}{7}} \quad (10)$$

Equations (9) and (10) are valid for values of $M \leq \frac{4}{21}$ (0.19), since for larger values of M, the maximum shock force occurs in the elastic phase of inflation.

Figures 9 and 10 illustrate the velocity and force profiles generated from equations (7) and (8) for initial projected area ratios of $\eta = 0$, and 0.2 with various mass ratios.

IV. Methods for Calculation of the Reference Time, t_o

The ratio concept is an ideal method to analyze the effects of the various parameters on the velocity and force profiles of the opening parachutes; however, a means of calculating t_o is required before specific values can be computed. Methods for computing the varying mass flow into the inflating canopy mouth, the varying mass flow out through the varying inflated canopy surface area, and the volume of air, V_o, which must be collected during the inflation process are required.

Figure 11 represents a solid cloth-type parachute canopy at some instant during inflation. At any given instant, the parachute drag area is proportional to the maximum inflated diameter. Also, the maximum diameter in conjunction with the suspension lines determines the inflow mouth area (A-A) and the pressurized canopy area (B-B-B). This observation provided the basis for the following assumptions. The actual canopy shape is of minor importance.

a. The ratio of the instantaneous mouth inlet area to the steady-state mouth area is in the same ratio as the instantaneous drag area.

$$\frac{A_M}{A_{Mo}} = \frac{C_D S}{C_D S_o}$$

b. The ratio of the instantaneous pressurized cloth surface area to the canopy surface area is in the same ratio as the instantaneous drag area.

$$\frac{S}{S_o} = \frac{C_D S}{C_D S_o}$$

c. Since the suspension lines in the unpressurized area of the canopy are straight, a pressure differential has not developed, and, therefore, the net airflow in this zone is zero.

Based on the foregoing assumptions, the mass flow equation can be written

$$dm = m\ \text{inflow} - m\ \text{outflow}$$

$$\rho \frac{dV}{dt} = \rho V A_M - \rho A_s P$$

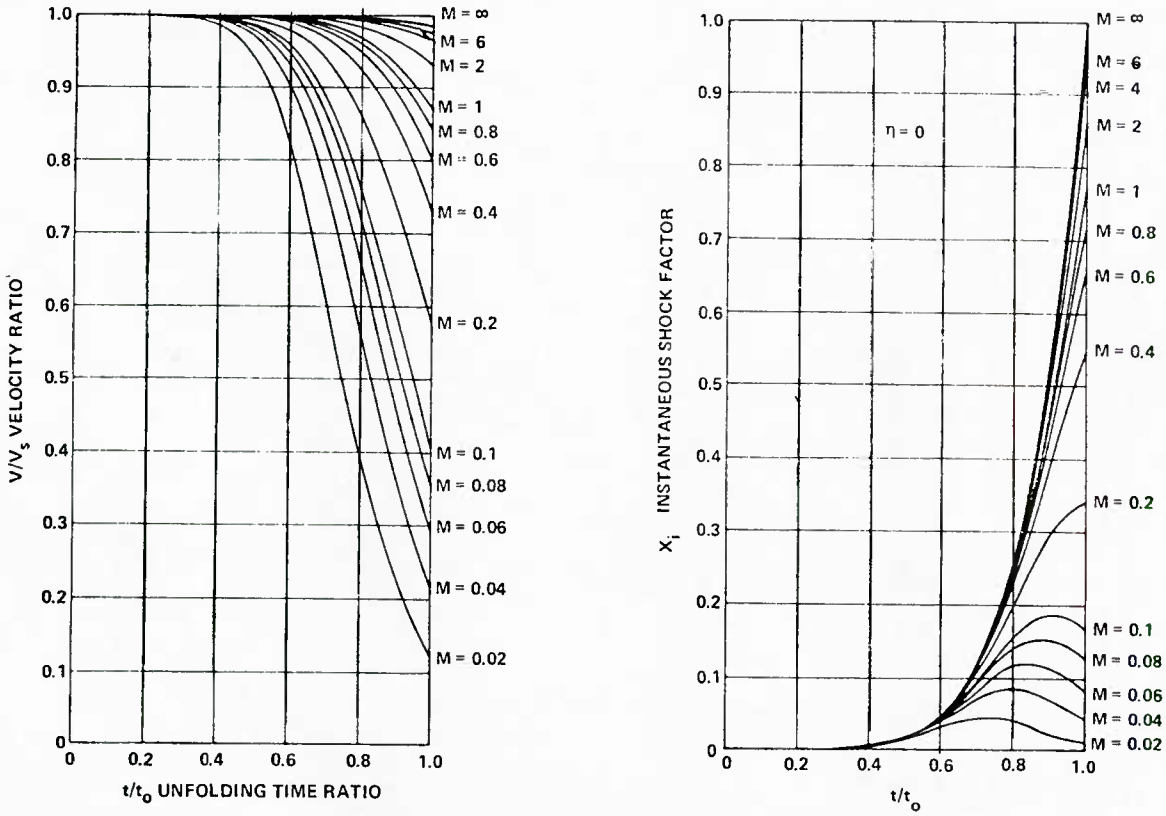

FIG. 9 EFFECT OF INITIAL AREA AND MASS RATIO ON THE SHOCK FACTOR AND VELOCITY RATIO DURING THE UNFOLDING PHASE FOR $\eta = 0$.

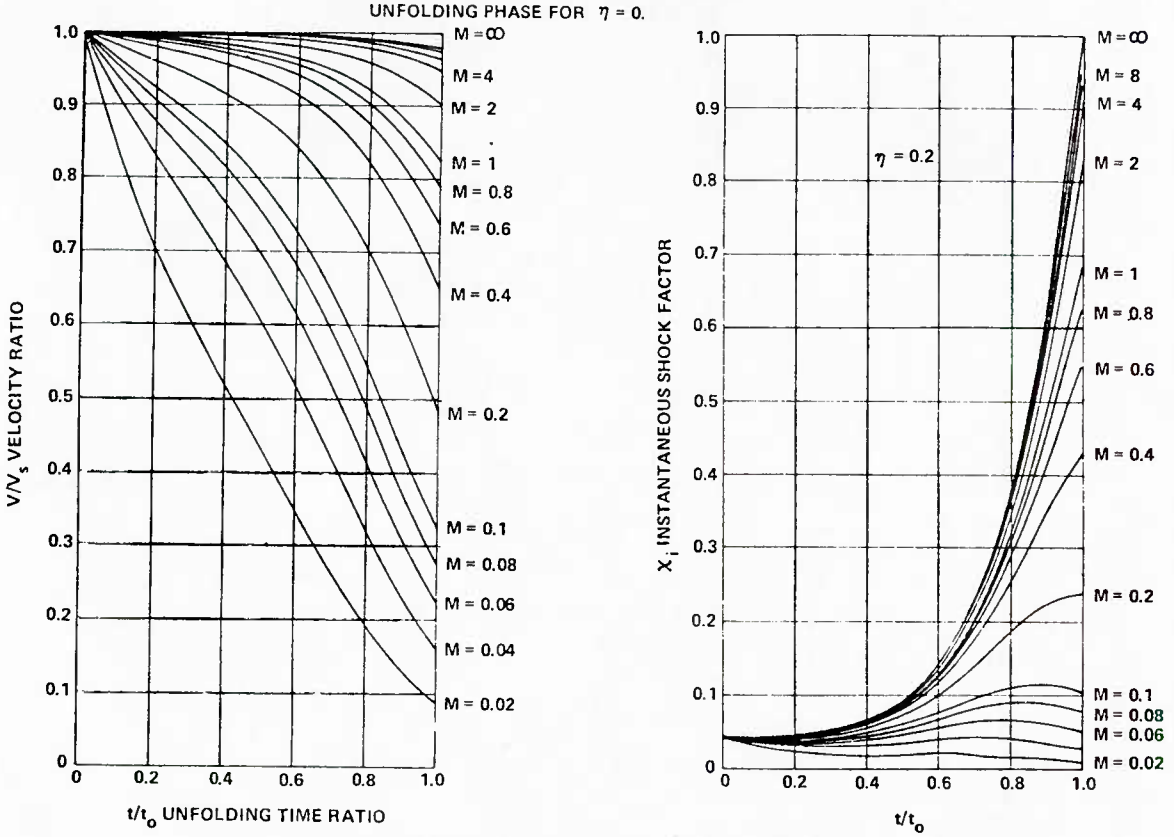

FIG. 10 EFFECT OF INITIAL AREA AND MASS RATIO ON THE SHOCK FACTOR AND VELOCITY RATIO DURING THE UNFOLDING PHASE FOR $\eta = 0.2$

$$\rho \frac{d\underline{V}}{dt} = \rho V A_{Mo} \frac{C_D S}{C_D S_o} - \rho A_{So} \frac{C_D S}{C_D S_o} P \qquad (11)$$

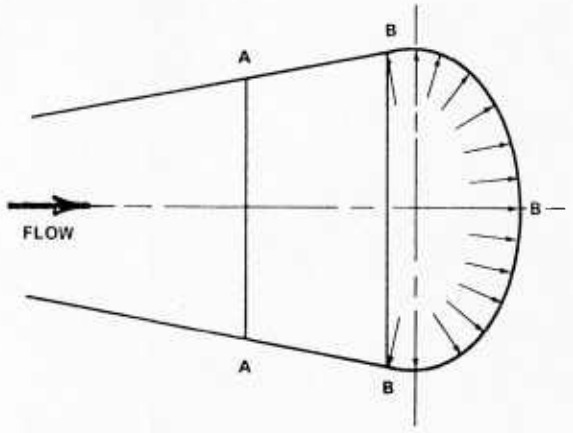

FIG. 11 PARTIALLY INFLATED PARACHUTE CANOPY

From equation (3)

$$\frac{C_D S}{C_D S_o} = \left(\frac{t}{t_o}\right)^6 \quad ; \text{ for } \eta = 0$$

From equation (7)

$$V = \frac{V_s}{1 + \frac{1}{7M}\left(\frac{t}{t_o}\right)^7} \quad ; \eta = 0$$

From equation (26)

$$P = k\left(\frac{C_P \rho}{2}\right)^n V^{2n}$$

$$\int_o^{\underline{V}_o} d\underline{V} = A_{Mo} V_s \int_o^{t_o} \frac{\left(\frac{t}{t_o}\right)^6}{1 + \frac{1}{7M}\left(\frac{t}{t_o}\right)^7} dt$$

$$-A_{So} k \left(\frac{C_P \rho}{2}\right)^n \int_o^{t_o} \left(\frac{t}{t_o}\right)^6 \left[\frac{V_s}{1 + \frac{1}{7M}\left(\frac{t}{t_o}\right)^7}\right]^{2n} dt \qquad (12)$$

Integrating:

$$\underline{V}_o = A_{Mo} V_s t_o M \ln\left[1 + \frac{1}{7M}\right]$$

$$-A_{So} k \left(\frac{C_P \rho}{2}\right)^n \int_o^{t_o} \left(\frac{t}{t_o}\right)^6 \left[\frac{V_s}{1 + \frac{1}{7M}\left(\frac{t}{t_o}\right)^7}\right]^{2n} dt \qquad (13)$$

Measured values of n indicate a data range from 0.574 through 0.771. A convenient solution to the reference time equation evolves when n is assigned a value of 1/2. Integrating equation (13) and using

$$V_s t_o M = \frac{2W}{g\rho C_D S_o}$$

$$\text{LET } K_1 = \frac{g\rho \underline{V}_o}{2W}\left[\frac{C_D S_o}{A_{Mo} - A_{So} k\left(\frac{C_P \rho}{2}\right)^{1/2}}\right]$$

$$t_o = \frac{14W}{g\rho V_s C_D S_o}\left[e^{K_1} - 1\right] \qquad (14)$$

Equation (14) expresses the unfolding reference time, t_o, in terms of mass, altitude, snatch velocity, airflow characteristics of the cloth, and the steady-state parachute geometry. Note that the term $g\rho\underline{V}_o/W$ is the ratio of the included air mass to the mass of the retarded hardware. Multiplying both sides of equation (14) by V_s demonstrates that

$$V_s t_o = \text{a constant which is a function of altitude}$$

Figures 12 and 13 indicate the parachute unfolding time and unfolding distance for values of n = 1/2 and n = 0.63246. Note the variation and convergence with rising altitude. The opening-shock force is strongly influenced by the inflation time. Because of this, the

value of t_o calculated by using a realistic value of n should be used in the lower atmosphere.

As an example of this method of opening-shock analysis, let us examine the effect of altitude on the opening-shock force of a T-10-type parachute retarding a 200-pound weight from a snatch velocity of V_s = 400 feet per second at sea level. Conditions of constant velocity and constant dynamic pressure are investigated. The results are presented in Figure 14. At low altitudes, the opening-shock force is less than the steady-state drag force; however, as altitude rises, the opening shock eventually exceeds the steady-state drag force at some altitude. This trend is in agreement with field test observations.

V. Correction of t_o for Initial Area Effects

The unfolding reference time, t_o, calculated by the previous methods assumes that the parachute inflates from zero drag area. In reality, a parachute has a drag

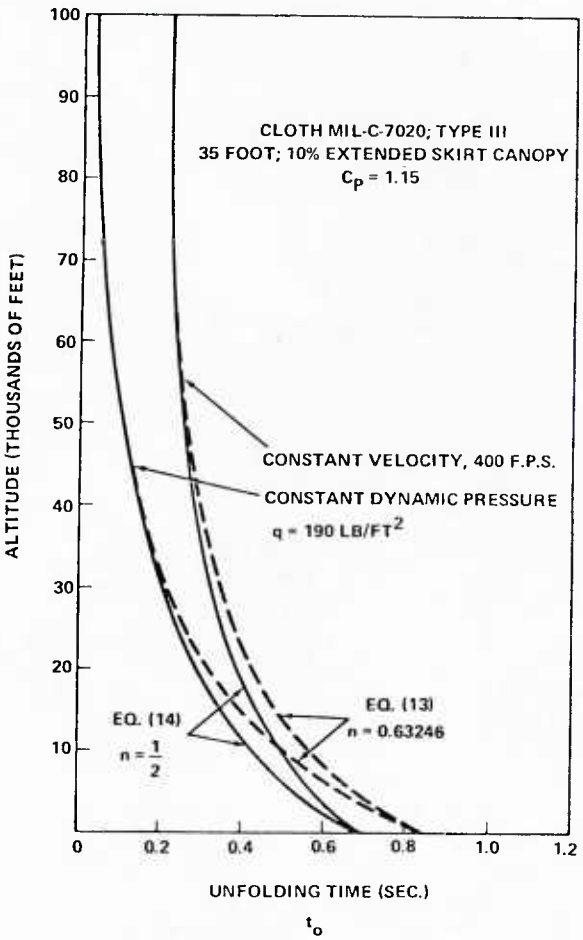

FIG. 12 EFFECT OF ALTITUDE ON THE UNFOLDING TIME "t_o" AT CONSTANT VELOCITY AND CONSTANT DYNAMIC PRESSURE FOR n = 1/2 AND n = 0.63296

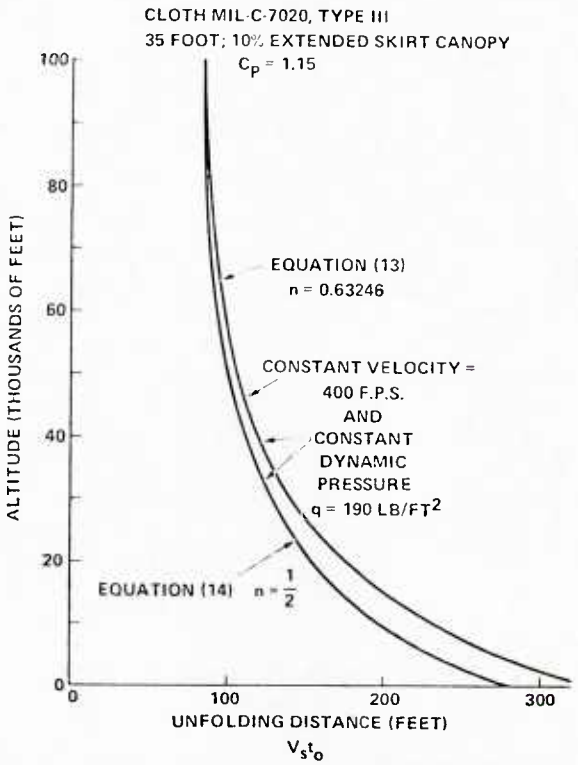

FIG. 13 EFFECT OF ALTITUDE ON THE UNFOLDING DISTANCE AT CONSTANT VELOCITY AND CONSTANT DYNAMIC PRESSURE FOR n = 1/2 AND n = 0.63246.

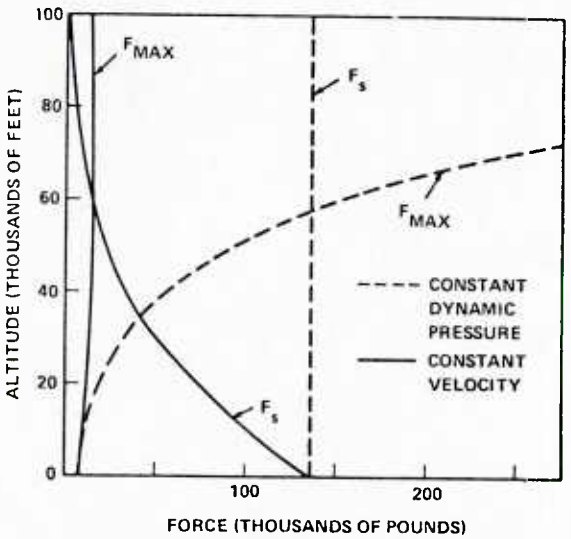

FIG. 14 VARIATION OF STEADY-STATE DRAG, F_s, AND MAXIMUM OPENING SHOCK WITH ALTITUDE FOR CONSTANT VELOCITY AND CONSTANT DYNAMIC PRESSURE

area at the beginning of inflation. Once t_o has been calculated, a correction can be applied, based upon what is known about the initial conditions.

Case A - When the initial projected area is known

$$\frac{A_i}{A_c} = \left(\frac{t_i}{t_o}\right)^3$$

$$t_i = \left(\frac{A_i}{A_c}\right)^{1/3} t_{o_{calculated}}$$

$$t_{o_{corrected}} = \left[1 - \left(\frac{A_i}{A_c}\right)^{1/3}\right] t_{o_{calculated}} \qquad (15)$$

Case B - When the initial drag area is known

$$\frac{C_D S_i}{C_D S_o} = \left(\frac{t_i}{t_o}\right)^6$$

$$t_i = \left(\frac{C_D S_i}{C_D S_o}\right)^{1/6} t_{o_{calculated}}$$

$$t_{o_{corrected}} = \left[1 - \left(\frac{C_D S_i}{C_D S_o}\right)^{1/6}\right] t_{o_{calculated}} \qquad (16)$$

The mass ratio should now be adjusted for the corrected t_o before velocity and force profiles are determined.

VI. Opening-Shock Force, Velocity Ratio, and Inflation Time During the Elastic Phase of Parachute Inflation

The mass ratio, M, is an important parameter in parachute analysis. For values of $M << 4/21$, the maximum opening-shock force occurs early in the inflation process, and the elastic properties of the canopy are not significant. As the mass ratio approaches $M = 4/21$, the magnitude of the opening-shock force increases, and the time of occurrence happens later in the deployment sequence. For mass ratios $M > 4/21$, the maximum shock force will occur after the reference time, t_o. Parachutes designed for high mass ratio operation must provide a structure of sufficient constructed strength, F_c, so that the actual elongation of the canopy under load is less than the maximum extensibility, ϵ_{max}, of the materials.

Development of the analysis in the elastic phase of inflation is similar to the technique used in the unfolding phase. Newton's second law of motion is used, together with the drag area ratio signature and mass ratio

$$\frac{C_D S}{C_D S_o} = \left(\frac{t}{t_o}\right)^6$$

which is still valid, as shown in Figure 7

$$\frac{1}{Mt_o}\int_{t_o}^{t}\left(\frac{t}{t_o}\right)^6 dt = V_s\int_{V_o}^{V}\frac{-dV}{V^2}$$

Integrating and solving for $\frac{V}{V_s}$

$$\frac{V}{V_s} = \frac{1}{\frac{V_s}{V_o} + \frac{1}{7M}\left[\left(\frac{t}{t_o}\right)^7 - 1\right]} \qquad (17)$$

where $\frac{V_o}{V_s}$ is the velocity ratio of the unfolding process at time $t = t_o$.

$$\frac{V_o}{V_s} = \frac{1}{1 + \frac{1}{M}\left[\frac{(1-\eta)^2}{7} + \frac{\eta(1-\eta)}{2} + \eta^2\right]} \qquad (18)$$

The instantaneous shock factor in the elastic phase becomes

$$x_i = \frac{C_D S}{C_D S_o}\left(\frac{V}{V_s}\right)^2$$

$$x_i = \frac{\left(\frac{t}{t_o}\right)^6}{\left[\frac{V_s}{V_o} + \frac{1}{7M}\left[\left(\frac{t}{t_o}\right)^7 - 1\right]\right]^2} \qquad (19)$$

The end point of the inflation process depends upon the applied loads, elasticity of the canopy, and the constructed strength of the parachute. A linear load elongation

relationship is utilized to determine the maximum drag area.

$$\frac{\epsilon}{F} = \frac{\epsilon_{max}}{F_c}$$

$$\epsilon = \frac{F\ \epsilon_{max}}{F_c} \qquad (20)$$

The force, F, is initially the instantaneous force at the end of the unfolding process

$$F = X_o F_s \qquad (21)$$

where X_o is the shock factor of the unfolding phase at $t = t_o$

$$X_o = \frac{1}{\left[1 + \frac{1}{M}\left[\frac{(1-\eta)^2}{7} + \frac{\eta(1-\eta)}{2} + \eta^2\right]\right]^2} \qquad (22)$$

Since the inflated shape is defined, the drag coefficient is considered to be constant, and the instantaneous force is proportional to the dynamic pressure and projected area. The maximum projected area would be developed if the dynamic pressure remained constant during the elastic phase. Under very high mass ratios, this is nearly the case over this very brief time period; but as the mass ratio decreases, the velocity decay has a more significant effect. The simplest approach for all mass ratios is to determine the maximum drag area of the canopy as if elastic inflation had occurred at constant dynamic pressure. Then utilizing the time ratio determined as an end point, intermediate shock factors can be calculated from equation (19) and maximum force assessed.

The initial force, $X_o F_s$, causes the canopy to increase in projected area. The new projected area in turn increases the total force on the canopy which produces a secondary projected area increase. The resulting series of events are resisted by the parachute materials. The parachute must, therefore, be constructed of sufficient strength to prevent the elongation of the materials from exceeding the maximum elongation.

$$\epsilon_o = \frac{X_o F_s}{F_c}\ \epsilon_{max} \qquad (23)$$

The next force in the series at constant q

$$F_1 = X_o F_s \frac{A_1}{A_c}$$

where

$$\frac{A_1}{A_c} = (1 + \epsilon_o)^2$$

Subsequent elongations in the system can be shown to be

$$\epsilon_1 = \epsilon_o\ (1 + \epsilon_o)^2$$

$$\epsilon_2 = \epsilon_o\ (1 + \epsilon_o\ (1 + \epsilon_o)^2)^2$$

The required canopy constructed strength can be determined for a given set of deployment conditions. The limiting value of the series (ϵ_ℓ) determines the end point time ratio.

$$\left(\frac{t_f}{t_o}\right)^6 = \frac{C_D S_{max}}{C_D S_o} = (1 + \epsilon_\ell)^2$$

$$\left(\frac{t_f}{t_o}\right) = \left(\frac{C_D S_{max}}{C_D S_o}\right)^{1/6} = (1 + \epsilon_\ell)^{1/3} \qquad (24)$$

Figure 15 illustrates the maximum drag area ratio as a function of ϵ_o.

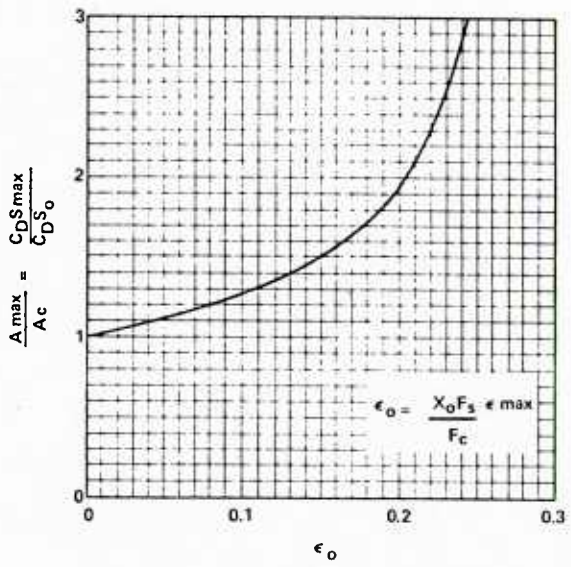

FIG. 15 MAXIMUM DRAG AREA RATIO VS. INITIAL ELONGATION

VII. Application of Cloth Permeability to the Calculation of the Inflation Time of Solid Cloth Parachutes

The mass outflow through the pressurized region of an inflating solid cloth parachute at any instant is dependent upon the canopy area which is subjected to airflow and the rate of airflow through that area. The variation of pressurized area as a function of reference time, t_o, was earlier assumed to be proportional to the instantaneous drag area ratio, leaving the rate-of-airflow problem to solve. The permeability parameter of cloth was a natural choice for determining the rate of airflow through the cloth as a function of pressure differential across the cloth. Heretofore, these data have been more of a qualitative, rather than quantitative, value. A new method of analysis was developed wherein a generalized curve of the form $P = k(\Delta P)^n$ was fitted to cloth permeability data for a number of different cloths and gives surprisingly good agreement over the pressure differential range of available data. The pressure differential was then related to the trajectory conditions to give a generalized expression which can be used in the finite mass ratio range, as well as the infinite mass case. The permeability properties were transformed into a mass flow ratio, M', which shows agreement with the effective porosity concept.

Measured and calculated permeability pressure data for several standard cloths are illustrated in Figure 16. This method has been applied to various types of cloth between the extremes of a highly permeable 3-momme silk to a relatively impervious parachute pack container cloth with reasonably good results, see Figure 17.

The canopy pressure coefficient, C_p, is defined as the ratio of the pressure differential across the cloth to the dynamic pressure of the free stream.

$$C_p = \frac{\Delta P}{q} = \frac{P(\text{internal}) - P(\text{external})}{1/2\ \rho V^2} \qquad (25)$$

where V is based on equation (7).

The permeability expression, $P = k(\Delta P)^n$ becomes

$$P = k\left(C_p \frac{\rho V^2}{2}\right)^n \qquad (26)$$

Although some progress has been made by Melzig and others on the measurement of the variation of the pressure coefficient on an actual inflating canopy, this dimension and its variation with time are still dark areas at the time of this writing. At the present time, a constant average value of pressure coefficient is used in these calculations. Figure 18 presents the effect of pressure coefficient and altitude on the unfolding time for constant deployment conditions.

It is well known that the inflation time of solid cloth parachutes decreases as the operational altitude increases. This effect can be explained by considering the ratio of the mass outflow through a unit cloth area to the mass inflow through a unit mouth area.

$$M' = \text{mass flow ratio} = \frac{\text{mass outflow}}{\text{mass inflow}}$$

where

$$\text{mass outflow} = P_{\rho}\ \frac{\text{slugs}}{\text{ft}^2\text{-sec}}\ (\text{per ft}^2\ \text{cloth area})$$

and

$$\text{mass inflow} = V_{\rho}\ \frac{\text{slugs}}{\text{ft}^2\text{-sec}}\ (\text{per ft}^2\ \text{inflow area})$$

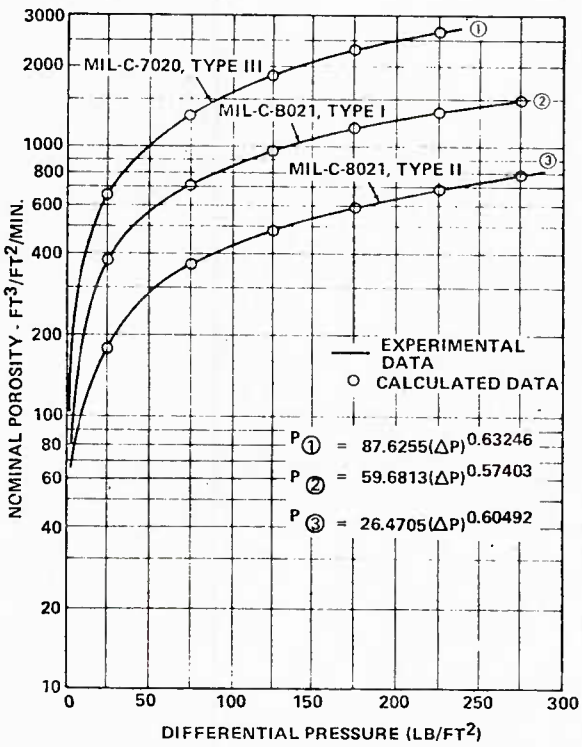

REPRODUCED FROM REFERENCE (4)

FIG. 16 NOMINAL POROSITY OF PARACHUTE MATERIAL VS DIFFERENTIAL PRESSURE.

Therefore, the mass flow ratio becomes

$$M' = \frac{P\rho}{V\rho} = \frac{P}{V}$$

$$M' = k\left(\frac{C_P\rho}{2}\right)^n V^{(2n-1)} \qquad (27)$$

Effective porosity, C, is defined as the ratio of the velocity through the cloth, u, to a fictitious theoretical velocity, v, which will produce the particular $\Delta P = 1/2\rho v^2$.

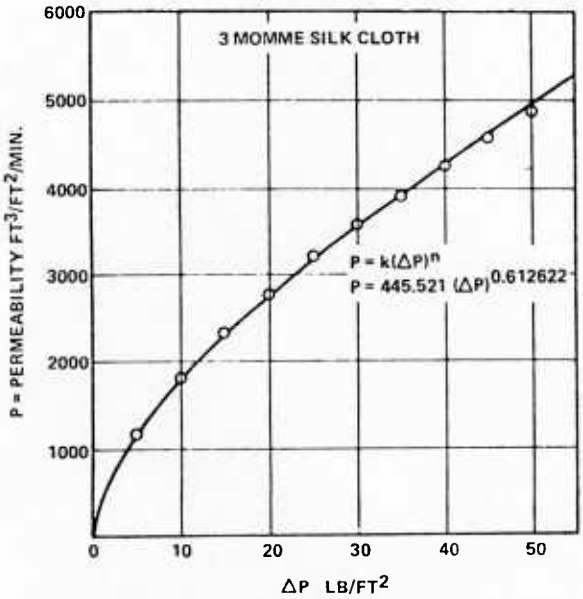

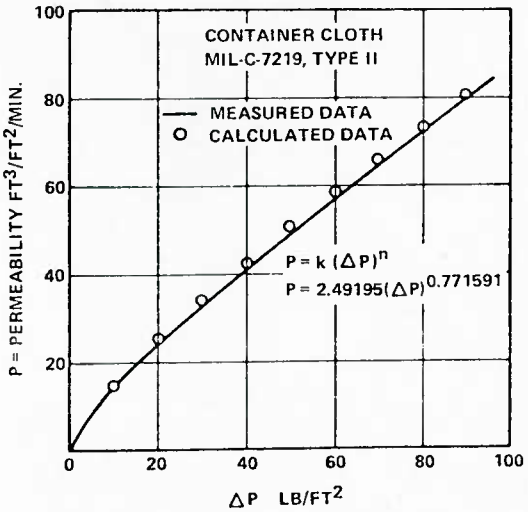

FIG. 17 COMPARISON OF MEASURED AND CALCULATED PERMEABILITY FOR RELATIVELY PERMEABLE AND IMPERMEABLE CLOTHS

AVERAGE CANOPY PRESSURE COEFFICIENT DURING INFLATION INCLUDING THE VENT

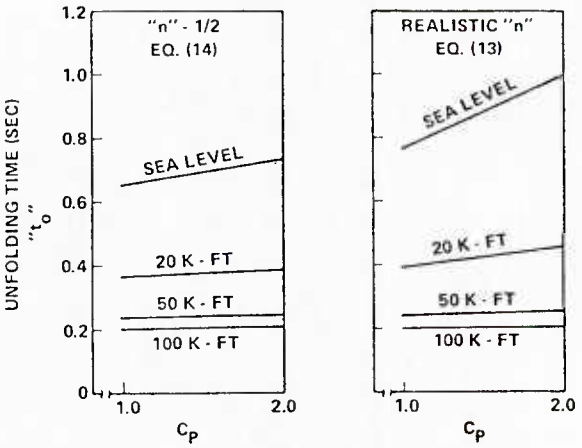

FIG. 18 EFFECT OF PRESSURE COEFFICIENT AND ALTITUDE ON THE UNFOLDING TIME.

$$\text{effective porosity, } C = \frac{u}{v} \qquad (28)$$

Comparison of the mass flow ratio and previously published effective porosity data is shown in Figure 19. The effects of altitude and velocity on the mass flow ratio are presented in Figures 20, and 21 for constant velocity and constant altitude. The decrease of cloth permeability with altitude is evident.

The permeability constants "k" and "n" can be determined from the permeability pressure differential data as obtained from an instrument such as a Frazier Permeameter. Two data points, "A" and

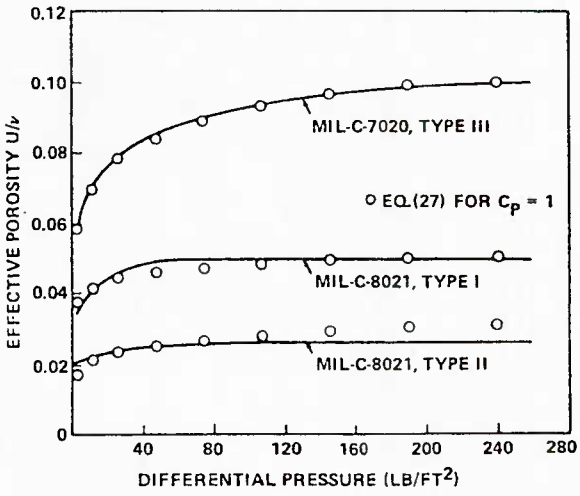

REPRODUCED FROM REFERENCE (4)

FIG. 19 THE EFFECTIVE POROSITY OF PARACHUTE MATERIALS VS. DIFFERENTIAL PRESSURE

"B," are selected in such a manner that point "A" is in a low-pressure zone below the knee of the curve, and point "B" is located in the upper end of the high-pressure zone, as shown in Figure 22.

The two standard measurements of 1/2 inch of water and 20 inches of water appear to be good data points if both are

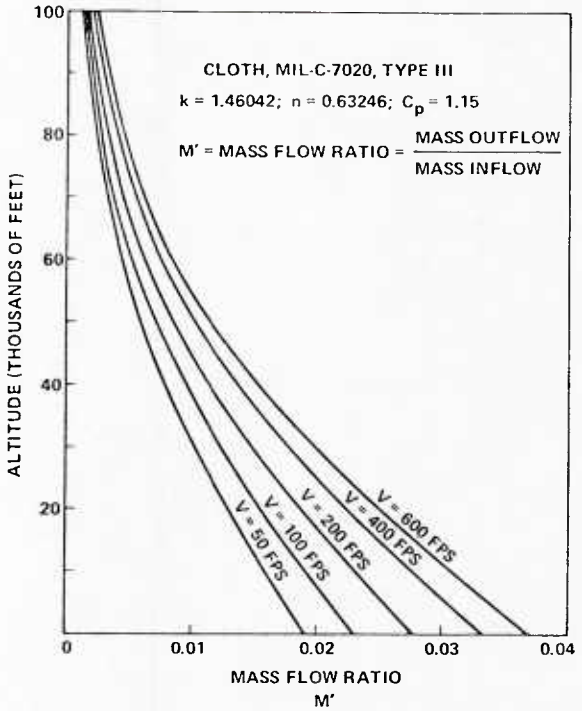

FIG. 20 EFFECT OF ALTITUDE ON MASS FLOW RATIO AT CONSTANT VELOCITY

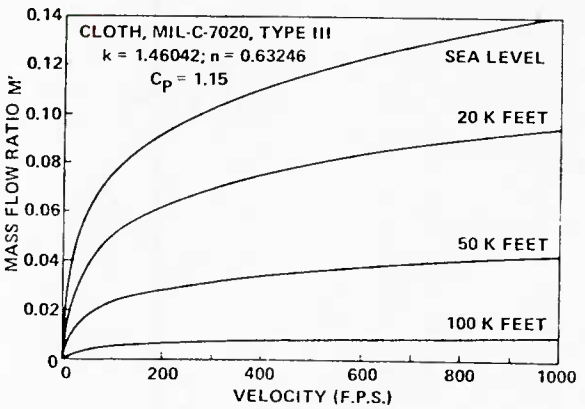

FIG. 21 EFFECT OF VELOCITY ON MASS FLOW RATIO AT CONSTANT DENSITY

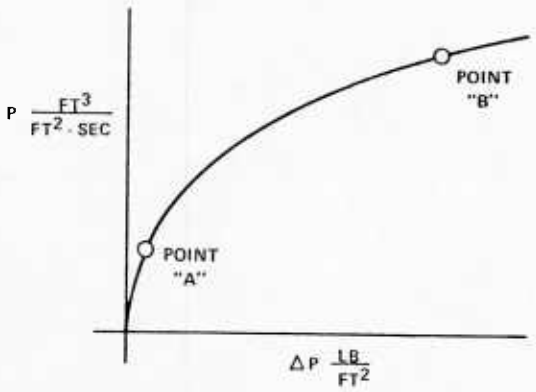

FIG. 22 LOCATION OF DATA POINTS FOR DETERMINATION OF "k" AND "n"

available on the same sample. Substituting the data from points "A" and "B" into $P = k(\Delta P)^n$:

$$n = \frac{\ell n\left(\frac{P_B}{P_A}\right)}{\ell n\left(\frac{\Delta P_B}{\Delta P_A}\right)} \qquad (29)$$

$$k = \frac{P_A}{(\Delta P_A)^n} = \frac{P_B}{(\Delta P_B)^n} \qquad (30)$$

VIII. Determination of the Parachute Included Volume and Associated Air Mass

Before the reference time, t_o, and inflation time, t_f, can be calculated, the volume of atmosphere, V_o, which is to be collected during the inflation process must be accurately known. This requirement dictates that a realistic inflated canopy shape and associated volume of atmosphere be determined. Figure 23 was reproduced from reference (5). The technique of using lampblack coated plates to determine the airflow patterns around metal models of inflated canopy shapes was used by the investigator of reference (5) to study the stability characteristics of contemporary parachutes, i.e., 1943. A by-product of this study is that it is clearly shown that the volume of air within the canopy bulges out of the canopy mouth (indicated by arrows) and extends ahead of the canopy hem. This volume must be collected during the inflation process. Another neglected, but significant, source of canopy volume exists in the billowed portion of the gore panels.

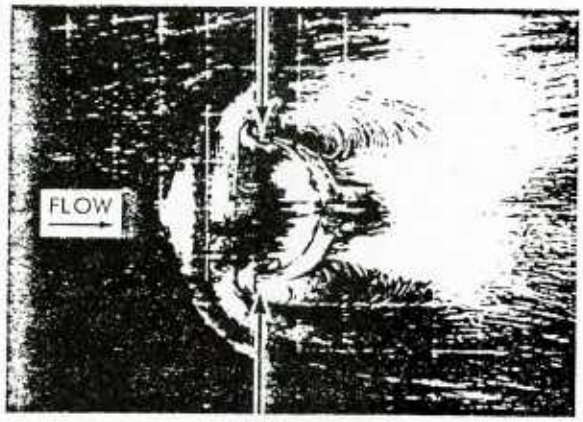

HEMISPHERE

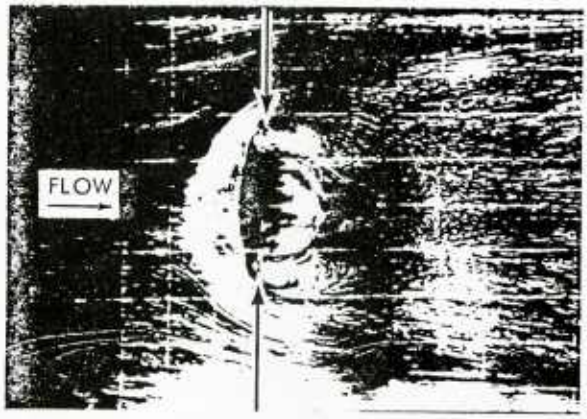

VENT PARACHUTE

REPRODUCED FROM REFERENCE (5)

FIG. 23 AIRFLOW PATTERNS SHOWING AIR VOLUME AHEAD OF CANOPY HEM

The steady-state canopy shape has been observed in wind-tunnel and field tests to be elliptical in profile. Studies of the inflated shape and included volume of several parachute types (flat circular, 10 percent extended skirt, elliptical, hemispherical, ring slot, ribbon, and cross) are documented in references (6) and (7). These studies demonstrated that the steady-state profile shape of inflated canopies of the various types can be approximated to be two ellipses of common major diameter, $2\bar{a}$, and dissimilar minor diameters, b and b', as shown in Figure 24. It was also shown that the volume of the ellipsoid of revolution formed by revolving the profile shape about the canopy axis was a good approximation of the volume of atmosphere to be collected during canopy inflation and included the air volume extended ahead of the parachute skirt hem together with the billowed gore volume.

$$\underline{V}_o = \frac{2}{3}\ \pi\bar{a}^3 \left[\frac{b}{\bar{a}} + \frac{b'}{\bar{a}}\right] \qquad (31)$$

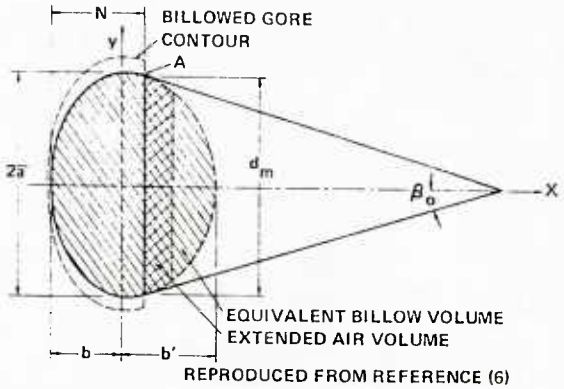

REPRODUCED FROM REFERENCE (6)

FIG. 24 PARACHUTE CROSS SECTION NOMENCLATURE

Tables I and II are summaries of test results reproduced from references (6) and (7), respectively, for the convenience of the reader.

IX. References

1. "A Method to Reduce Parachute Inflation Time with a Minor Increase in Opening Force," WADD Report TR 60-761
2. Berndt, R. J., and DeWesse, J. H., "Filling Time Prediction Approach for Solid Cloth Type Parachute Canopies," AIAA Aerodynamic Deceleration Systems Conference, Houston, Texas, 7-9 Sep 1966
3. "Theoretical Parachute Investigations," Progress Report No. 4, Project No. 5, WADC Contract AF33 (616)-3955, University of Minnesota
4. "Performance of and Design Criteria for Deployable Aerodynamic Decelerators," TR ASK-TR-61-579, AFFDL, AIRFORCESYSCOM, Dec 1963
5. "Investigation of Stability of Parachutes and Development of Stable Parachutes from Fabric of Normal Porosity," Count Zeppelin Research Institute Report No. 300, 23 Mar 1943
6. Ludtke, W. P., "A New Approach to the Determination of the Steady-State Inflated Shape and Included Volume of Several Parachute Types," NOLTR 69-159, 11 Sep 1969
7. Ludtke, W. P., "A New Approach to the Determination of the Steady-State Inflated Shape and Included Volume of Several Parachute Types in 24-Gore and 30-Gore Configurations," NOLTR 70-178, 3 Sep 1970

TABLE I SUMMARY OF PARACHUTE SHAPE TEST RESULTS FOR 12-GORE AMD 16-GORE CONFIGURATIONS

Parachute Type	No. of Gores	Suspension Line Length inches	Velocity mph	Velocity fps	Scale Factor, K $\frac{2\bar{a}}{D_o}$	$\frac{2\bar{a}}{D_F}$	$\frac{2\bar{a}}{D_R}$	$\frac{2\bar{a}}{L}$	$\frac{N}{\bar{a}}$	Axes Ratio $\frac{b}{\bar{a}}$	$\frac{b'}{\bar{a}}$	$\frac{b}{\bar{a}}+\frac{b'}{\bar{a}}$	Volume in^3 V_H	V_C	V_o	$\frac{V_o}{V_H}$
Flat Circular	12	34	50	73	.645	.650			.856	.6115	.8817	1.4932	4476	4481	6980	1.56
	16	34	50	73	.663	.669			.820	.5558	.9039	1.4597	4450	4100	7325	1.65
10% Extended Skirt	12	34	100	147	.663	.652			.881	.6424	.8860	1.5284	3928	4400	6783	1.73
	16	34	17	25	.654	.640			.785	.5580	.8502	1.4082	4051	3920	6197	1.53
Elliptical	12	34	75	110			.916		.812	.5626	.9657	1.5283		3322	5405	
	16	34	17	25			.875		.800	.6169	8163	1.4332		2726	4405	
Hemispherical	12	34	125	183			.996		1.254	1.0005	.9080	1.9085		6224	8666	
	16	34	75	110			.994		1.185	.9129	.9380	1.8509		5921	8370	
Ringslot 16% Geometric Porosity	12	34	25	37	.607	.654			.853	.6566	.8735	1.530	3800	3650	5903	1.55
	12	34	100	147	.616	.663			.922	.6566	.8735	1.530	3800	4198	6166	1.62
	12	34	200	293	.637	.686			.918	.6566	.8735	1.530	3800	4624	6826	1.90
	16	34	25	37	.611	.658			.827	.6004	.8890	1.4894	3800	3763	5685	1.50
	16	34	100	147	.617	.664			.864	.6004	.8890	1.4894	3800	3985	6030	1.59
	16	34	200	293	.645	.695			.844	.6004	.8890	1.4894	3800	4430	6897	1.82
Ribbon 24% Geometric Porosity	12	34	25	37	.586	.632			.859	.6558	.8768	1.5326	3800	3323	5335	1.40
	12	34	100	147	.615	.663			.837	.6558	.8768	1.5326	3800	3714	6163	1.62
	12	34	200	293	.632	.681			.877	.6558	.8768	1.5326	3800	4280	6683	1.76
	16	34	25	37	.603	.650			.797	.5570	.8578	1.4148	3800	3438	5358	1.41
	16	34	100	147	.626	.674			.791	.5570	.8578	1.4148	3800	3804	5983	1.57
	16	34	200	293	.648	.698			.781	.5570	.8578	1.4148	3800	4164	6656	1.75
Cross Chute W/L = .264		34	25	37	.710			.543	1.242	.8867	1.2776	2.1643	1928	3768	5798	3.01
		34	100	147	.707			.540	1.270	.8867	1.2776	2.1643	1928	3810	5712	2.96
		34	200	293	.716			.547	1.285	.8867	1.2776	2.1643	1928	4212	5925	3.07
		47	25	37	.759			.580	1.113	.8494	1.2512	2.1006	1928	4052	6868	3.56
		47	100	147	.729			.557	1.205	.8494	1.2512	2.1006	1928	3973	5958	3.09
		47	200	293	.775			.592	1.110	.8494	1.2512	2.1006	1928	4292	7303	3.79

REPRODUCED FROM REFERENCE (6)

TABLE II SUMMARY OF PARACHUTE SHAPE TEST RESULTS FOR 24-GORE AND 30-GORE CONFIGURATIONS

Parachute Type	No. of Gores	Suspension Line Length inches	Velocity mph	Velocity fps	Scale Factor, K $\frac{2\bar{a}}{D_o}$	$\frac{2\bar{a}}{D_F}$	$\frac{N}{\bar{a}}$	Axes Ratio $\frac{b}{\bar{a}}$	$\frac{b'}{\bar{a}}$	$\frac{b}{\bar{a}}+\frac{b'}{\bar{a}}$	Volume in^3 V_H	V_c	V_o	$\frac{V_o}{V_H}$
Flat Circulars	24	34	50	73	.677	.679	.795	.5758	.8126	1.3884	4362	4695	7273	1.67
	30	34	17	25	.668	.669	.827	.6214	.7806	1.4020	4342	4626	7027	1.62
10% Extended* Skirt	24	34	100	147	.665	.648	.834	.5949	.8771	1.4720	4138	4446	6930	1.67
	30	34	17	25	.650	.633	.825	.6255	.7962	1.4127	4172	4076	6265	1.50
Ring Slot 16% Geometrically Porous	24	34	25	37	.663	.665	.824	.5800	.9053	1.4853	3591	3878	6031	1.68
	24	34	100	147	.680	.682	.819	.5800	.9053	1.4853	3591	4079	6510	1.81
	24	34	200	293	.694	.696	.809	.5800	.9053	1.4853	3591	4270	6924	1.93
	30	34	25	37	.677	.678	.788	.5800	.9053	1.4853	3582	3826	6404	1.79
	30	34	100	147	.684	.685	.802	.5800	.9053	1.4853	3582	4023	6588	1.84
	30	34	200	293	.698	.699	.800	.5800	.9053	1.4853	3582	4260	7012	1.96
Ribbon 24% Geometrically Porous	24	34	25	37	.671	.673	.770	.5980	.8187	1.4167	3591	3591	5968	1.66
	24	34	100	147	.676	.678	.813	.5980	.8187	1.4167	3591	3927	6097	1.70
	24	34	200	293	.687	.689	.804	.5980	.8187	1.4167	3591	4061	6389	1.78
	30	34	25	37	.655	.657	.782	.6021	.8463	1.4484	3582	3396	5666	1.58
	30	34	100	147	.669	.670	.784	.6021	.8463	1.4484	3582	3622	6022	1.68
	30	34	200	293	.677	.679	.823	.6021	.8463	1.4484	3582	4002	6256	1.75

*Since this parachute was "breathing" during the test, several photographs were taken at each speed. The data were reduced from the photograph which most reasonably appeared to represent the equilibruim state.

REPRODUCED FROM REFERENCE (7)

X. List of Symbols

A_c - Steady-state projected area of the inflated parachute, ft^2

A_M - Instantaneous canopy mouth area, ft^2

A_{Mo} - Steady-state inflated mouth area, ft^2

a - Acceleration, ft/sec^2

$2\bar{a}$ - Maximum inflated parachute diameter of gore mainseam, ft

b - Minor axis of the ellipse bounded by the major axis ($2\bar{a}$) and the vent of the canopy, ft

b' - Minor axis of the ellipse which includes the skirt hem of the canopy, ft

C - Effective porosity

C_D - Parachute coefficient of drag

C_p - Parachute pressure coefficient, relates internal and external pressure (ΔP) on canopy surface to the dynamic pressure of the free stream

D_o - Nominal diameter of the aerodynamic decelerator = $\sqrt{4S_o/\pi}$, ft

F - Instantaneous force, lbs

F_s - Steady-state drag force that would be produced by a fully open parachute at velocity V_s, lbs

F_c - Constructed strength of the parachute, lbs

F_{max} - Maximum opening-shock force, lbs

g - Gravitational acceleration, ft/sec^2

k - Permeability constant of canopy cloth

m - Mass, slugs

M - Mass ratio - ratio of the mass of the retarded hardware (including parachute) to a mass of atmosphere contained in a right circular cylinder of length ($V_s t_o$), face area ($C_D S_o$), and density (ρ)

M' - Mass flow ratio - ratio of atmosphere flowing through a unit cloth area to the atmosphere flowing through a unit inlet area at arbitrary pressure

n - Permeability constant of canopy cloth

P - Cloth permeability - rate of airflow through a cloth at an arbitrary differential pressure, $ft^3/ft^2/sec$

q - Dynamic pressure, lb/ft^2

$S = A_s$ - Instantaneous inflated canopy surface area, ft^2

$S_o = A_{so}$ - Canopy surface area, ft^2

t - Instantaneous time, sec

t_o - Reference time when the parachute has reached the design drag area for the first time, sec

t_f - Canopy inflation time when the inflated canopy has reached its maximum physical size, sec

u - Air velocity through cloth in effective porosity, ft/sec

v - Fictitious theoretical velocity used in effective porosity, ft/sec

V - Instantaneous system velocity, ft/sec

V_o - System velocity at the time $t = t_o$, ft/sec

V_s - System velocity at the end of suspension line stretch, ft/sec

$\underline{V}_o$ - Volume of air which must be collected during the inflation process, ft^3

W - Hardware weight, lb

x_1 - Instantaneous shock factor

X_o - Shock factor at the time $t = t_o$

ρ - Air density, $slugs/ft^3$

η - Ratio of parachute projected mouth area at line stretch to the steady-state projected area

ϵ - Instantaneous elongation

ϵ_{max} - Maximum elongation

ϵ_o - Initial elongation at the beginning of the elastic phase of inflation

S.F. - Parachute safety factor = F_c/F_{max}

Appendix B

A GUIDE FOR THE USE OF APPENDIX A

At first reading, Appendix A may appear to be a complicated system of analysis because of the many formulae presented. Actually, once understood, the technique is straightforward and uncomplicated. The author has attempted to simplify the algebra wherever possible. This appendix presents, in semi-outline form, a guide to the sequence of calculations because the analysis does require use of formulae from the text, not necessarily in the order in which they were presented. Also, the user can be referred to graphs of performance to illustrate effects.

In order to compute t_o, other parameters must be obtained from various sources.

I. Determine System Parameters

1. $C_D S_o$, drag area, ft^2 obtained from design requirement.

2. V_s, fps, velocity of system at suspension line stretch.

3. ρ, slugs/ft^3, air density at deployment altitude.

4. W, lb, system weight (including weight of the parachute) from design requirements.

5. $\underline{V}_o$, ft^3, this volume of air, which is to be collected during inflation, is calculated from the steady-state inflated shape geometry of the particular parachute type. The nomenclature is described in Figure 24, p. A-14. When D_o or D_F is known, $\bar{a}$ can be calculated from data in Table I and Table II, p. A-15, for various parachute types and number of gores. Then the geometric volume $\underline{V}_o$ can be calculated by Equation (31), p. A-14, with appropriate values of $b/\bar{a}$ and $b'/\bar{a}$ from the tables.

6. A_{MO}, ft^2, steady-state canopy mouth area

$$A_{MO} = \pi \bar{a}^2 \left[1 - \left(\frac{N/\bar{a} - b/\bar{a}}{b'/\bar{a}} \right)^2 \right] \qquad \text{(B-1)}$$

where $N/\bar{a}$, $b/\bar{a}$, and $b'/\bar{a}$ are available from Tables I and II for the particular type of parachute and number of gores.

7. A_{so}, ft^2, canopy surface area $= \frac{\pi}{4} D_o^2$

8. C_p, pressure coefficient, see Figure 18, p. A-12. A constant $C_p = 1.7$ for all altitudes seems to yield acceptable results.

9. Constants k and n are derived from measurements of the air flow through the cloth. Only k is needed for Equation (14), but n is also required for Equation (13). These parameters can be determined for any cloth using the technique described beginning on p. A-12. The two-point method is adequate if the ΔP across the cloth is in the range of ΔP for actual operation. Check-points of cloth permeability can be measured and compared to calculated values to verify agreement. If the data are to be extrapolated to operational ΔP's greater than measured, a better method of determining k and n from the test data would be a least squares fit through many data points. This way errors due to reading either of the two points are minimized.

II. Step 1

Calculate the reference time t_o by use of Equations (13) or (14), p. A-7. If the deployment altitude is 50,000 feet or higher, Equation (14) is preferred due to its simplicity. For altitudes from sea level to 50,000 feet, Equation (13) is preferred. Figure 12, p. A-8, shows the effect of altitude on t_o and can be taken as a guide for the user to decide whether to use Equation (13) or (14). One should keep in mind that the opening shock force can be a strong function of inflation time, so be as realistic as possible. If Equation (13) is elected, the method in use at the NSWC/WO is to program Equation (13) to compute the parachute volume, $\underline{V}_o$, for an assumed value of t_o. Equation (14), because of its simplicity, can be used for a first estimate of t_o at all altitudes. The computed canopy volume is then compared to the canopy volume calculated from the geometry of the parachute as per Equation (31), p. A-14. If the volume computed from the mass flow is within the volume computed from the geometry within plus or minus a specified delta volume, the time t_o is printed out. If not within the specified limits, t_o is adjusted, and a new volume calculated. For a 35-foot D_o, T-10 type canopy, I use plus or minus 10 cubic feet in the volume comparison. The limit would be reduced for a parachute of smaller D_o.

If $\underline{V}_o$ calculated $= \underline{V}_o$ geometry $\pm$ 10, then print answer.

If $\underline{V}_o$ calculated $\neq \underline{V}_o$ geometry $\pm$ 10, then correct t_o as follows:

$$t_o = t_o \frac{\underline{V}_{o\ \text{geometry}}}{\underline{V}_{o\ \text{calculated}}} \qquad \text{(B-2)}$$

The new value of t_o is substituted in the "do loop" and the volume recomputed. This calculation continues until the required volume is within the specified limits.

III. Calculate t_o corrected for initial area. The t_o of Section II assumes that the parachute inflated from a zero initial area. If this is a reasonable assumption for the particular system under study, then the mass ratio can be determined from Equation (6), p. A-4. For $\eta = 0$ if the value of $M \leq 0.19$, then a finite state of deployment exists, and the time ratio of occurrence and the maximum shock factor can be determined from Equations (9) and (10), respectively, on p. A-5. If $\eta \neq 0$, then the limiting mass ratio for finite operations will rise slightly as described in Appendix C. Figures C-1 and C-2 illustrate the effects of initial area on limiting mass ratios and shock factors respectively. If the mass ratio is greater than the limiting mass ratio (M_L), then the maximum shock force occurs at a time greater than t_o and the elasticity of the materials must be considered (see Section VI).

If $\eta \neq 0$, then the reference time, t_o, will be reduced, and the mass ratio will rise due to partial inflation at the line stretch. Figures 9 and 10, p. A-6, illustrate the effects of initial area on the velocities and shock factor during the "unfolding" inflation. Equation (15), p. A-9, can be used to correct t_o calculated for the cases where $\eta = Ai/Ac$. If the initial value of drag area is known, Equation (16), p. A-9, can be used to correct t_o and rechecked for limiting mass ratios versus η in Appendix C.

IV. Opening shock calculations in the elastic phase of inflation. It has been considered that from time $t = 0$ to $t = t_o$ the parachute has been inelastic. At the time $t = t_o$ the applied aerodynamic load causes the materials to stretch and the parachute canopy increases in size. The increased size results in an increase in load, which causes further growth, etc. This sequence of events continues until the applied forces have been balanced by the strength of materials. The designer must insure that the constructed strength of the materials is sufficient to resist the applied loads for the material elongation expected. Use of materials of low elongation should result in lower opening shock forces as $C_D S_{max}$ is reduced.

When the mass ratio of the system is greater than the limiting mass ratio, the elasticity of the materials and material strength determine the maximum opening shock force. The maximum elongation ε_{max} and the ultimate strength of the materials are known from tests or specifications. The technique begins on p. A-9.

At the time $t = t_o$, calculate the following quantities for the particular values of M and η.

a. V_o/V_s from Equation (18), p. A-9.

b. X_o from Equation (22), p. A-10.

c. ε_o from Equation (23), p. A-10.

d. Determine $C_D S_{max}/C_D S_O$ from Figure 15, p. A-10.

e. Calculate the inflation time ratio t_f/t_o from Equation (24), p. A-10.

f. Calculate the maximum shock factor from Equation (19), p. A-9.

g. Calculate the opening shock force $F_{max.} = X_i F_S$ where

$$F_S = \frac{1}{2}\rho V_S^2 C_D S_o$$

h. Calculate filling time, t_f(sec)

$$t_f = t_o \left(\frac{t_f}{t_o}\right)$$

V. In order to simplify the required effort, the work sheets of Table B-1 are included on pages B-5 through B-9 to aid the engineer in systematizing the analysis. The work sheets should be reproduced to provide additional copies.

Table B-1. Opening Shock Force

CALCULATION WORK SHEETS

	SYMBOL	VALUE	DIMENSION
1. Parachute type -			
2. System parameters			
a. System weight, W (lb)	W		lb.
b. Gravity, g (ft/sec^2)	g		ft/sec^2
c. Deployment altitude (ft)			ft.
d. Deployment air density, ρ (slugs/ft^3)	ρ		slugs/ft^3
e. Velocity at line stretch, V_s (fps)	V_s		fps.
f. Steady state canopy data			
(1) Diameter, D_o (ft)	D_o		ft.
(2) Inflated diameter, $2\bar{a}$ (ft); $\frac{2\bar{a}}{D_o}$ = *	$2\bar{a}$		ft.
(3) Surface area, S_o (ft^2); $\frac{\pi}{4} D_o^2$	$A_{so} = S_o$		ft.^{2}
(4) Drag area, $C_D S_o$ (ft^2); $C_D \times S_o$	$C_D S_o$		ft.^{2}
(5) Mouth area, A_{MO}^* (ft^2) $A_{MO} = \pi \bar{a}^2 \left[1 - \left(\frac{N/\bar{a} - b/\bar{a}}{b'/\bar{a}}\right)^2\right]$	A_{MO}		ft.^{2}
(6) Volume, V_o* (ft^3) $V_o = \frac{2}{3} \pi \bar{a}^3 \left[\frac{b}{\bar{a}} + \frac{b'}{\bar{a}}\right]$	V_o		ft.^{3}
g. Cloth data			
(1) k } Calculate using technique beginning on p. A-12.	k		—
(2) n } Note: Permeability is usually measured as ft^3/ft^2/min. For these calculations permeability must be expressed as ft^3/ft^2/sec	n		—

* Data for these calculations are listed in Tables 1 and 2, p. A-15.

Table B-1. Opening Shock Force (cont'd)

	SYMBOL	VALUE	DIMENSION
(3) ε_{max}; determine maximum elongations from pull test data of joints, seams, lines, etc. Use minimum ε_{max} determined from tests.			
(4) Cp; pressure coefficient	C_p		—
h. Steady state drag, F_S (lb), $F_S = \frac{1}{2}\rho V_S^2 C_D S_o$	F_s		lb.
i. Parachute constructed strength, F_C (lb); determined from data on efficiency of seams, joints, lines. Constructed strength is the minimum load required to fail a member times the number of members.	F_c		lb.
3. Force calculations			
a. Calculate t_o for $\eta = 0$; eq. 14, p. A-7. $t_o = \frac{14W}{\rho g V_S C_D S_o}\left[\epsilon^{\frac{\rho g V_o}{2W}\left[\frac{C_D S_o}{A_{MO} - A_{SO}\, k\left(\frac{C_P \rho}{2}\right)^{\frac{1}{2}}}\right]} - 1\right]$	t_o		sec.
Check Figure 13, p. A-8, for advisability of using eq. 13, p. A-7.			
b. If $\eta = 0$, proceed with steps c through e. If $\eta \neq 0$, go to step f.			
c. Mass ratio, M; eq. 6, p. A-4 $M = \frac{2W}{\rho g V_S t_o C_D S_o}$	M		—
d. If $M \leq 4/21$ for $\eta = 0$, then finite mass deployment is indicated.			
(1) Time ratio at $x_{i\ max}$; eq. 9, p. A-5 $\frac{t}{t_{o\,@\,x_{i_{max}}}} = \left(\frac{21M}{4}\right)^{\frac{1}{7}}$	$\frac{t}{t_{o\,@\,x_{i_{max}}}}$		—
(2) Max shock factor, x_i; eq., 10, p. A-5 $x_{i_{max}} = \frac{16}{49}\left(\frac{21M}{4}\right)^{\frac{6}{7}}$	$x_{i_{max}}$		—

Table B-1. Opening Shock Force (Cont'd)

	SYMBOL	VALUE	DIMENSION
(3) Max shock force, F_{max} (lb) $F_{max.} = \chi_{i\ max.} F_S$	F_{max}		lb.
e. If M > 4/21; then intermediate mass or infinite mass deployment is indicated and the elasticity of materials is involved. Calculate the trajectory conditions at time $t = t_o$.			
(1) Velocity ratio @ $t = t_o$ for $\eta = 0$ $\frac{V_o}{V_S} = \frac{1}{1 + \frac{1}{7M}}$	$\frac{V}{V_o}$		–
(2) Shock factor X_o @ $t = t_o$ for $\eta = 0$ $X_o = \frac{1}{\left[1+\frac{1}{7M}\right]^2} = \left(\frac{V_o}{V_S}\right)^2$	X_o		–
(3) Initial elongation, ε_o; eq. 23, p. A-10 $\epsilon_o = \frac{X_o F_S}{F_c} \epsilon_{max}$	ϵ_o		–
(4) Determine $\frac{C_D S_{max}}{C_D S_o}$ from Figure 15, p. A-10	$\frac{C_D S_{max}}{C_D S_o}$		–
(5) Calculate inflation time ratio, $\frac{t_f}{t_o}$; eq. 24, p. A-10 $\frac{t_f}{t_o} = \left(\frac{C_D S_{max}}{C_D S_o}\right)^{\frac{1}{6}}$	$\frac{t_f}{t_o}$		–
(6) Calculate maximum shock factor, $\chi_{i\ max}$; eq. 19, p. A-9 $\chi_{i_{max}} = \frac{\left(\frac{t_f}{t_o}\right)^6}{\left[\frac{V_S}{V_o} + \frac{1}{7M}\left[\left(\frac{t_f}{t_o}\right)^7 - 1\right]\right]^2}$	$\chi_{i_{max}}$		–
(7) Calculate maximum shock force, F_{max} (lb), $F_{max} = \chi_{i_{max}} F_S$	F_{max}		lb.

Table B-1. Opening Shock Force (cont'd)

	SYMBOL	VALUE	DIMENSION
(8) Inflation time, sec = $t_f = t_o \left(\frac{t_f}{t_o}\right)$	t_f		Sec.
f. If $\eta \neq 0$, correct t_o for initial area effects; eq. 16, p. A-9 $t_o = \left[1 - \left(\frac{C_D S_i}{C_D S_o}\right)^{1/6}\right] t_{o\ calculated}$	t_o		Sec.
g. Mass Ratio, M, eq. 6, p. A-4 $M = \frac{2W}{\rho g V_s t_o C_D S_o}$	M		—
h. Calculate limiting mass ratio, M_L $M_L = \frac{1}{3(1-\eta)} - \left[\frac{9}{14}\eta^2 + \frac{3}{14}\eta + \frac{1}{7}\right]$	M_L		—
If $M \leq M_L$, finite mass deployment is indicated and $x_{i\ max}$ can be determined by eq. 8, p. A-5 by assuming values of t/t_o and plotting the data using the methods of Appendix C.			
i. If $M > M_L$, then intermediate mass or infinite mass deployment is indicated and the elasticity of materials is involved. Calculate the trajectory conditions at time $t = t_o$.			
(1) Velocity ratio @ $t = t_o$ for $\eta \neq 0$; eq. 18, p. A-9 $\frac{V_o}{V_S} = \frac{1}{\left[1 + \frac{1}{M}\left[\frac{(1-\eta)^2}{7} + \frac{\eta(1-\eta)}{2} + \eta^2\right]\right]}$	$\frac{V_o}{V_s}$		—
(2) Shock factor X_o @ $t = t_o$ for $\eta \neq 0$; eq. 22, p. A-10 $X_o = \frac{1}{\left[1 + \frac{1}{M}\left[\frac{(1-\eta)^2}{7} + \frac{\eta(1-\eta)}{2} + \eta^2\right]\right]^2} = \left(\frac{V_o}{V_S}\right)^2$	X_o		—
(3) Initial elongation, ϵ_o; eq. 23, p. A-10 $\epsilon_o = \frac{X_o F_S}{F_c}\ \epsilon_{max}$	ϵ_o		—
(4) Determine $\frac{C_D S_{max}}{C_D S_o}$ from Figure 15, p. A-10	$\frac{C_D S_{max}}{C_D S_o}$		—

Table B-1. Opening Shock Force (Contd

	SYMBOL	VALUE	DIMENSION
(5) Calculate inflation time ratio, $\frac{t_f}{t_o}$; eq. 24, p. A-10 $\frac{t_f}{t_o} = \left(\frac{C_D S_{max}}{C_D S_o}\right)^{\frac{1}{6}}$	$\frac{t_f}{t_o}$		–
(6) Calculate maximum shock factor, $x_{i\ max}$; eq. 19, p. A-9 $\chi_{i_{max}} = \frac{\left(\frac{t_f}{t_o}\right)^6}{\left[\frac{V_S}{V_o} + \frac{1}{7M}\left[\left(\frac{t_f}{t_o}\right)^7 - 1\right]\right]^2}$	$\chi_{i_{max}}$		–
(7) Calculate maximum shock force, F_{max}(lb) $F_{max} = \chi_{i_{max}} F_S$	F_{max}		lb.
(8) Calculate inflation time, t_f(sec) $t_f = t_o \left(\frac{t_f}{t_o}\right)$	t_f		Sec.

DISTRIBUTION

	Copies
Commander Naval Air Systems Command Attn: Library Department of the Navy Washington, DC 20361	4
Commander Naval Sea Systems Command Attn: Library Washington, DC 20362	4
Commanding Officer Naval Personnel Research and Development Center Attn: Library Washington, DC 20007	2
Office of Naval Research Attn: Library Washington, DC 20360	4
Office of Naval Research Attn: Fluid Dynamics Branch Structural Mechanics Branch 800 N. Quincy St. Arlington, VA 22217	2
Director Naval Research Laboratory Attn: Code 2027 Library, Code 2029 (ONRL) Washington, DC 20375	2
U.S. Naval Academy Attn: Library Annapolis, MD 21402	2
Superintendent U.S. Naval Postgraduate School Attn: Library (Code 0384) Monterey, CA 93940	2
Commander U.S. Naval Air Development Center Attn: Library William B. Shope David N. DeSimone Louis A. Daulerio Thomas J. Popp Maria C. Hura Warminster, PA 18974	2 1 1 1 1 1
Commanding Officer U.S. Naval Weapons Support Center Attn: Library Mark T. Little Crane, IN	2 1
Commander Naval Ship Research and Development Center Attn: Library Washington, DC 20007	2

	Copies
Commander U.S. Naval Missile Center Attn: Technical Library, Code N0322 Point Mugu, CA 93041	2
Director Marine Corps Development and Education Command Development Center Attn: Library Quantico, VA 22134	2
Marine Corps Liaison Officer U.S. Army Natick Laboratories Natick, MA 01760	2
Commanding General U.S. Army Mobility Equipment Research and Development Center Attn: Technical Document Center Fort Belvoir, VA 22660	2
Commanding General U.S. Army Aviation Systems Command Attn: Library St. Louis, MO 63166	2
Commanding General U.S. Army Munitions Command Attn: Technical Library Stanley D. Kahn Dover, NJ 07801	2 1
Commanding General U.S. Army Weapons Command Attn: Technical Library Research and Development Directorate Rock Island, IL 61201	2
Commanding General U.S. Army ARDEC Attn: Library Walt Koenig SMCAR-AET-A Roy W. Kline SMCAR-AET-A Dover, NJ 07801	2 1 1
Army Research and Development Laboratories Aberdeen Proving Ground Attn: Technical Library, Bldg. 313 Aberdeen, MD 21005	2
Commanding General Edgewood Arsenal Headquarters Attn: Library Aero Research Group Aberdeen Proving Ground Aberdeen, MD 21005	2
Commanding General Harry Diamond Laboratories Attn: Technical Library 2800 Powder Mill Road Adelphi, MD 20783	2

DISTRIBUTION (cont.)

	Copies
U.S. Army Ballistic Research Laboratories Attn: Technical Library Aberdeen Proving Ground Aberdeen, MD 21005	2
Commanding General U.S. Army Foreign Science and Technology Center Attn: Technical Library 220 Seventh Street, NE Federal Building Charlottesville, VA 22312	2
Commanding General U.S. Army Material Command Attn: Library Washington, DC 20315	2
Commanding General U.S. Army Test and Evaluation Command Attn: Library Aberdeen Proving Ground Aberdeen, MD 21005	2
Commanding General U.S. Army Combat Developments Command Attn: Library Fort Belvoir, VA 22060	2
Commanding General U.S. Army Combat Developments Command Institute of Advanced Studies Attn: Technical Library Carlisle Barracks, PA 17013	2
Commanding General U.S. Army Material Laboratories Attn: Technical Library Fort Eustis, VA 23604	2
U.S. Army Air Mobility R&D Laboratory Eustis Directorate Attn: Systems and Equipment Division Fort Eustis, VA 23604	2
President U.S. Army Airborne Communications and Electronics Board Fort Bragg, NC 28307	2
U.S. Army CDC Institute of Land Combat Attn: Technical Library 301 Taylor Drive Alexandria, VA 22314	2
Commanding General U.S. Army Missile Command Redstone Scientific Information Center Attn: Library Redstone Arsenal, AL 35809	2
U.S. Army Natick Laboratories Liaison Office Attn: Library Aeronautical Systems Division Wright Patterson Air Force Base, OH 45433	2
Army Research Office Attn: Library Box CM, Duke Station Durham, NC 27706	2
Office of the Chief of Research and Development Department of the Army Attn: Library Washington, DC 20310	2

	Copies
U.S. Army Advanced Material Concepts Agency Department of the Army Attn: Library Washington, DC 20315	2
Director U.S. Army Mobility R&D Laboratory AMES Research Center Attn: Library Moffett Field, CA 94035	2
Commandant Quartermaster School Airborne Department Attn: Library Fort Lee, VA 23801	2
U.S. Army Standardization Group, UK Attn: Research/General Material Representative Box 65 FPO, NY 09510	2
Commanding Officer McCallan AFB Attn: Library SA-ALC/MMIR CA 95652	2
Arnold Engineering Development Center (ARO, Inc.) Attn: Library/Documents Arnold Air Force Station, TN 37389	2
NASA Lewis Research Center Attn: Library, Mail Stop 60-3 21000 Brookpark Road Cleveland, OH 44135	1
NASA John F. Kennedy Space Center Attn: Library, Code IS-CAS-42B Kennedy Space Center, FL 32899	1
NASA Manned Spacecraft Center Attn: Library, Code BM6 2101 Webster Seabrook Road Houston, TX 77058	1
NASA Marshall Space Flight Center Attn: Library Huntsville, AL 25812	1
NASA Goddard Space Flight Center/ Wallops Flight Facility Attn: Library Mr. Mendle Silbert Mr. Earl B. Jackson, Code 841.2 Mr. Dave Moltedo, Code 841.2 Mr. Anel Flores Wallops Island, VA 23337	2 1 1 1 1
National Aeronautics and Space Administration Attn: Library Headquarters, MTG 400 Maryland Avenue, SW Washington, DC 20456	2
Defense Advanced Research Projects Agency Attn: Technical Library 1400 Wilson Boulevard Arlington, VA 22209	2
Director Defense Research and Engineering Attn: Library (Technical) The Pentagon Washington, DC 20301	2

DISTRIBUTION (cont.)

	Copies
Director of Defense Research and Engineering Department of Defense Washington, DC 20315	2
Defense Technical Information Center Cameron Station Alexandria, VA 22304-6145	12
Library of Congress Attn: Gift and Exchange Division Washington, DC 20540	4
University of Minnesota Dept. of Aerospace Engineering Attn: Dr. W. L. Garrard Minneapolis, MN 55455	2
Sandia National Laboratories Attn: Code 1632	2
Library	2
Dr. Dean Wolf	1
Dr. Carl Peterson	10
R. Kurt Baca	1
Ira T. Holt	1
Donald W. Johnson	1
James W. Purvis	1
Harold E. Widdows Albuquerque, NM 87185	1
Applied Physics Laboratory The Johns Hopkins University Attn: Document Librarian Johns Hopkins Road Laurel, MD 20810	2
National Academy of Sciences National Research Council Committee on Undersea Warfare Attn: Library 2101 Constitution Ave., N.W. Washington, DC 20418	2
Sandia Corporation Livermore Laboratory Attn: Technical Reference Library P.O. Box 969 Livermore, CA 94551	2
Lockheed Missiles and Space Company Attn: Mr. K. French P.O. Box 504 Sunnyvale, CA 94086	1
Rockwell International Corporation Space and Information Systems Division Attn: Technical Information Center 12214 S. Lakewood Boulevard Downey, CA 90241	2
PA State University Applied Research Laboratory Attn: Library P.O. Box 30 State College, PA 16801	2
Honeywell, Incorporated Attn: Mr. S. Sopczak 600 Second Street N. Hopkins, MN 55343	1
National Bureau of Standards Attn: Library Washington, DC 20234	2

Internal Distribution:	Copies
U13 (C. J. Diehlmann)	1
U13 (W. P. Ludtke)	25
U13 (J. F. McNelia)	1
U13 (D. W. Fiske)	1
U13 (J. Murphy)	1
U13 (J. G. Velez)	1
U13 (J. Correll)	1
U13 (S. Hunter)	1
U13 (M. L. Fender)	1
U13 (R. L. Pense)	1
U13 (M. L. Lama)	1
U43 (J. Rosenberg)	1
U43 (B. Delre)	1
E231	2
E232	15
E31 (GIDEP Office)	1